REPUBLIC OF TÜRKİYE

ALTINBAŞ UNIVERSITY

Institute of Graduate Studies

Civil Engineering

ASSESMENT OF THE DYNAMIC PROPERTIES AND RESPONSE OF MASONRY MINARETS IN ISTANBUL

Mohamad AL-ASWAD

Master's Thesis

Supervisor

Assoc. Prof. Dr. Aykut ERKAL

Istanbul, 2023

ASSESMENT OF THE DYNAMIC PROPERTIES AND RESPONSE OF MASONRY MINARETS IN ISTANBUL

Mohamad AL-ASWAD

Civil Engineering

Master's Thesis

ALTINBAŞ UNIVERSITY

2023

The thesis titled ASSESMENT OF THE DYNAMIC PROPERTIES AND RESPONSE OF MASONRY MINARETS IN ISTANBUL prepared by MOHAMAD AL-ASWAD and submitted on 23/08/2023 has been **accepted unanimously** for the degree of Master of Science in Civil Engineering.

Assoc. Prof. Dr. Aykut ERKAL

Supervisor

Thesis Defense Committee Members:

Assoc. Prof. Dr. Aykut ERKAL	Department of Civil Engineering, Altınbaş University	
Asst. Prof. Dr. Mohsen SEYEDİ	Department of Civil Engineering, Altınbaş University	
Assoc. Prof. Dr. Hakkı ORAL ÖZHAN	Department of Civil Engineering, Yeditepe University	

I hereby declare that this thesis meets all format and submission requirements of a Master's thesis.

Submission date of the thesis to Institute of Graduate Studies: ___/___/___

I hereby declare that all information/data presented in this graduation project has been obtained in full accordance with academic rules and ethical conduct. I also declare all unoriginal materials and conclusions have been cited in the text and all references mentioned in the Reference List have been cited in the text, and vice versa as required by the abovementioned rules and conduct.

Mohamad AL-ASWAD

Signature

ABSTRACT

ASSESMENT OF THE DYNAMIC PROPERTIES AND RESPONSE OF MASONRY MINARETS IN ISTANBUL

Al-ASWAD, Mohamad

M.Sc., Civil Engineering, Altınbaş University,

Supervisor: Assoc. Prof. Dr. Aykut ERKAL

Date: August / 2023

Pages: 64

Over the centuries, numerous Islamic minarets have been constructed in various forms, the Ottoman minarets were one of them. In this study, seven Ottoman minarets located in Istanbul were evaluated, 5 of them were constructed using stone masonry, and the rest were constructed using both stone masonry and brickwork. Firstly, the physical and mechanical properties of the materials used were determined using a Schmidt hammer test. Regression analysis was conducted to investigate the relationship between the fundamental period and the affected parameters. In this study, two equations were derived to estimate the fundamental period for minarets. The seven minarets were analyzed under their self-weight, time history analysis, and modal analysis using the SAP2000 software.

Keywords: Minarets, Regression Analysis, Schmidt Hammer Test, Time History Analysis, Modal Analysis.

TABLE OF CONTENTS

LIST OF TABLES

Pages

LIST OF FIGURES

ABBREVIATIONS

MPMR : Modal Participating Mass Ratio

LIST OF SYMBOLS

f (Hz)	:	Frequency
T	:	Fundamental Period
A	:	Cross-Sectional Area
I	:	Moment Of Inertia
H	:	Effective Height
E	:	Modulus of Elasticity
P	:	Density
$N_{Average}$	:	Average Rebound Numbers
F_c	:	Compressive Strength of Units
F_{cm}	:	Compressive Strength of Masonry
F_t	:	Tensile Strength
R	:	Correlation Coefficient
R^2	:	Coefficient of Determination

1. INTRODUCTION

The Ottoman minarets hold significant historical value and exhibit unique architectural features. They consist of several main components: a foot, a boot section, and a transitional segment that connects the boot to the main body of the minaret. The main body of the minaret typically has a polygonal shape, and in the body section, there is a balcony that decorates the upper part of the minaret. Above the balcony, there is the upper body of the minaret, followed by the spire and a beautiful end ornament. Inside the minaret, there is a spiral staircase supported by a strong core. This combination of elements showcases the architectural brilliance of the Ottoman era. Unfortunately, many of the Ottoman minarets in Istanbul have succumbed to destructive earthquakes over the years, most notably in 1766. Typically, Ottoman minarets are attached to mosque. For this study, seven minarets were carefully selected. Figure 1.1 shows the height details of the minarets, ranging from the shortest at 19.48m to the tallest at a height of 74.51m, along with cross sections of the bottom of the polygonal body.

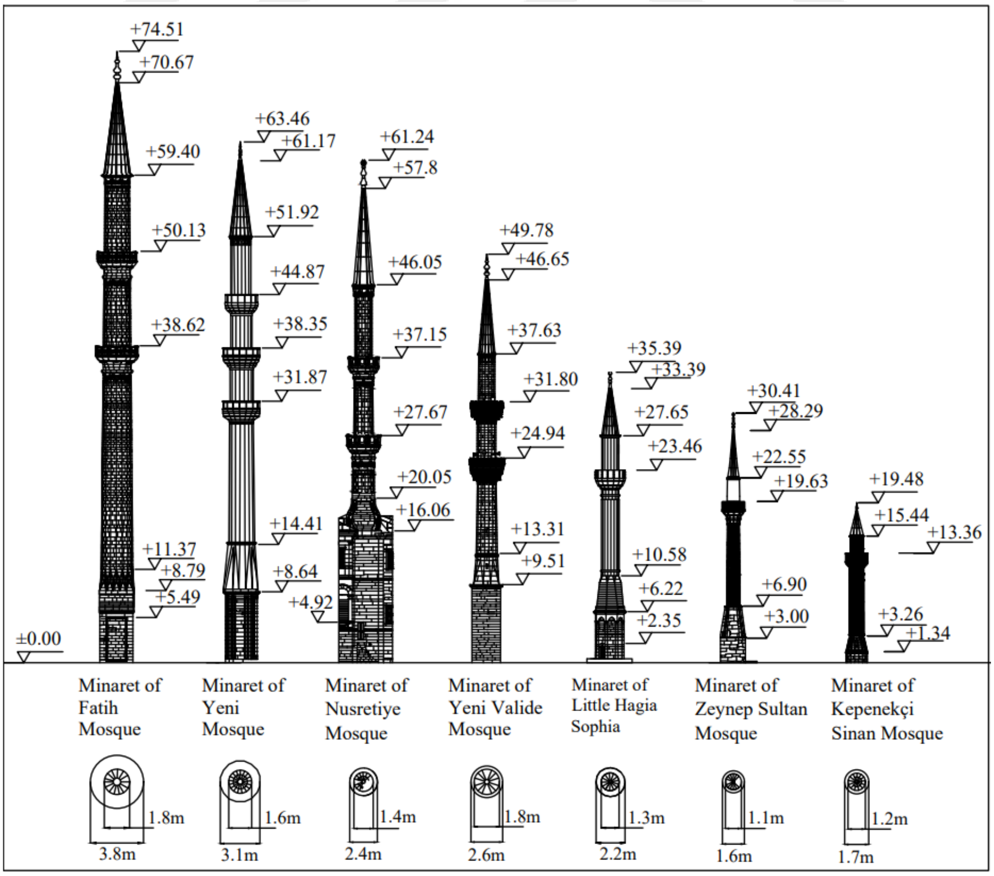

Figure 1.1: The Seven Historical Minarets.

2. GENERAL INFORMATION

During this study 7 historical Ottoman minarets were studied. Table 2.1 shows the characteristics of the minarets.

Table 2.1: The Characteristics of the Minarets.

Minaret	Fatih Mosque	Yeni Mosque	Nusretiye Mosque	Yeni Valide Mosque	Little Hagia Sophia Mosque	Zeynep Sultan Mosque	Kepenekçi Sinan Mosque
Height (m)	74.51	63.46	61.24	49.78	35.39	30.41	19.48
Number of Balconies	2	3	2	2	1	1	1
Boot Dimensions (m)	4.14×4.01	4.98×4.33	3.00×2.95	3.20×3.00	D=3.1	3.64×3.08	D=2.74
Diameter of Polygonal Body (m)	3.80	2.83	1.98	2.58	2.10	1.57	1.73
Diameter of the Lowest Balcony (m)	5.21	4.64	3.64	4.08	3.55	2.75	2.75
Height of Transitional Segment (m)	2.58	5.77	3.99	3.80	4.36	3.90	1.92
Height of Spire (m)	11.27	9.24	11.75	9.02	5.74	5.74	3.04
Year of Construction	1463-1470	1597-1663	1823-1826	1708-1710	527–536	1769	1546
Attached or Unattached to the Mosque	Attached	Attached	Attached	Attached	Unattached	Attached	Attached
Constituent Materials	Stone Masonry	Stone Masonry	Stone Masonry	Stone Masonry	Stone Masonry	Brick and Stone Masonry	Brick and Stone Masonry

2.1 MINARET OF FATIH MOSQUE

Istanbul's conquest was an important historical event in world history. The Fatih Mosque and its complex were among the earliest incredible works of Ottoman Turkish architecture that were built and constructed in Istanbul (Figure 2.1). Fatih Mosque and its complex were constructed between 1463 and 1470 by the architect Sinânüddin Yusuf bin Abdullah in the Fatih district in Istanbul. The complex consists of schools, a clinic, a library, and tombs. The 16-line Arabic inscription on both sides and above the gate indicates the date of construction. The inscription was created by Ali bin Sofi, a popular calligrapher of that era. The names of the ancestors of Fatih Sultan Mehmed Han through the lineage to Osman bey are stated in the inscription. The mosque has been exposed to several earthquakes in the past, the most serious occurred in 1766. On the third day of Eid Al-Adha in 1766, the mosque collapsed as a result of the earthquake, as well as its huge dome and the top section of the minarets. The mosque was repaired by the architect Mehmed Tahir Ağa and the restoration work was finished in 1771. Two minarets stand on the right and the left of the mosque. The minarets were restored in a wavy baroque design and decorated with ornate carvings. The minaret's stone spires were replaced in 1965 by lead-coated wooden spires [1].

Figure 2.1: Fatih Mosque.

2.2 MINARET OF YENI MOSQUE

The Yeni Mosque bears the classical Ottoman architectural style with its plan scheme, construction techniques, materials, and decorations (Figure 2.2). The Yeni Mosque is located in Eminönü district. The construction was started in 1597 during the reign of Sultan III. Mehmed Han, by the architect Davut Ağa. The mosque is located at sea level, which caused the groundwater to flow to the mosque's foundation level. The architect used large piles for the foundation. Although the occurrence of many earthquakes until these days, the foundation has not been affected. That indicates the solidity of the work. The construction works were finished in 1663 by the architect Mustafa Ağa. The Yeni Mosque has a large dome in the center supported by four columns and surrounded by four half-domes. The mosque consists of a courtyard, a harem, and a fountain. Two minarets are located on the northwest corner of the mosque. Each of the minarets has three balconies. The entry to the minarets is accessible through the mosque's side corridors. The minaret's spires are lead coated. The Yeni Mosque was repaired Between 2007 and 2009 [1].

Figure 2.2: Yeni Mosque.

2.3 MINARET OF NUSRETIYE MOSQUE

The Nusretiye Mosque was built during the reign of Sultan II. Mahmud Han in Tophane area. The Nusretiye Mosque was designed and constructed by architect Krikor Amira Balyan. The construction started in 1823 and was completed in 1826. The mosque's architecture combines both imperial and baroque designs. The Nusretiye Mosque has a very attractive stone structure with a single dome 14 meters in diameter and 33 meters in height (Figure 2.3). The candlesticks of the mosque are made of green stone. The courtyard of the mosque is paved with marble. Due to the lack of visibility of Ramadan mahyasi from the sea, the two beautiful minarets, up to the lower balconies were demolished after the completion of their construction and rebuilt higher than it was. The transition segment of the minarets is leaf-decorated and pear-shaped. The polygonal body is rising on the pear-shaped transition segment. The minarets have wavy balconies and long conical spires [2].

Figure 2.3: Nusretiye Mosque.

2.4 MINARET OF YENI VALIDE MOSQUE

The Yeni Valide Mosque, tombs, school, and fountain are all parts of the Yeni Valide Complex. The Yeni Valide Complex is one of the complexes that formed the basis of Ottoman social life. The structure is located northwest of Mihrimah Sultan Mosque in Üsküdar. The complex was established on a rectangle shape area. The complex was constructed by the architect Mehmet Ağa. According to the inscription on the gate, the construction started in 1708 and was completed in 1710. Yeni Valide Mosque has two minarets, which are regarded as the last example of classical Ottoman style and each has two balconies (Figure 2.4), located at the corners where the mosque and the last prayer hall meet. The wooden entrance doors of the two minarets, located at the last prayer hall, open into the corridor at the main entrance of the mosque. The minarets were built of limestone. There is an unadorned transition segment between the boot section and the polygonal body of the minarets [3].

Figure 2.4: Yeni Valide Mosque.

2.5 MINARET OF LITTLE HAGIA SOPHIA MOSQUE

Justinian started constructing the Little Hagia Sophia Mosque as a church (Church of SS Sergius and Bacchus) in 527 and completed it in 536. In 1510, the church was converted into a mosque (Figure 2.5). The church has 5 domes. The last prayer hall, a muezzin mahfili (a raised platform in a mosque from which the Quran is recited and where the muezzin chants), minber, and mihrab were added to the mosque later. A single minaret standing separately from the mosque was built in 1762. The little Hagia Sophia Mosque has dimensions of 30m x 34m. The dome high is 19m. The last prayer hall has five arches and a dome above it. The minaret was partially destroyed in 1940 and was repaired using limestone in 1956 [4].

Figure 2.5: Little Hagia Sophia Mosque.

2.6 MINARET OF ZEYNEP SULTAN MOSQUE

The Zeynep Sultan Mosque is located in the Alemdar area, directly across the street from Gülhane Park. It was built by Zeynep Sultan. A school, tombs, and a fountain are located adjacent to the mosque, constituting a small complex. According to the inscriptions that are in the mosque, the mosque was built in 1769, and the architect was Mehmed Tahir Ağa. Zeynep Sultan Mosque was constructed with traditional materials from stone masonry and brickwork. It has a square design with one dome that sits on the walls. The school is located behind the mosque and is still utilized by the Ministry of Awqaf until these days. The mosque has a minaret with a single balcony (Figure 2.6). The Ministry of Awqaf restored the mosque in 1958, and the prayers restored it in 1983 [1].

Figure 2.6: Zeynep Sultan Mosque.

2.7 MINARET OF KEPENEKÇI SINAN MOSQUE

The Kepenekçi Sinan Mosque is located in Eminönü district. Hoca Sinan constructed the Kepenekçi Sinan Mosque in 1546. The mosque has an area of 207 square meters. The walls of the mosque are made of limestone. The roof of the mosque and the minbar are made of wood. A marble arch frames the lower windows, which are rectangular in design. The upper windows are constructed in a beehive shape. The ascent to the top section is provided through wooden stairs. The mosque is divided into two parts, has two mihrabs and the interior is accessed by two separate doors. The mosque has a single minaret on the right front. The minaret has a single balcony in which the boot section and the transition segment are attached to the mosque and made of limestone masonry, while the polygonal body is made of brickwork masonry (Figure 2.7). After several restorations, the mosque was finally repaired by Fatih Mosque Protection Association in 1968 [1].

Figure 2.7: Kepenekçi Sinan Mosque.

3. LITERATURE REVIEW

Regression analysis is a type of analysis that establishes a link between variables to generate a mathematical equation. Regression analysis can be linear or nonlinear. There are many previous studies on regression analysis to estimate the fundamental period, such as Oliveira et al (2012), and (Serhatoğlu and Livaoğlu (2019)). Many researchers in previous studies investigate different equations to estimate the fundamental period or frequency for structures that have tower shape. Some equations consist only of geometric properties variables. for example, the equations of Oliveira et al (2012), Serhatoğlu and Livaoğlu (2019), Faccio et al, Rainieri and Fabbrocino, Ministerio de Fomento, and Shakya. On the other hand, some equations include both geometric properties variables and material properties variables like the equation of Serhatoğlu and Livaoğlu (2019).

The Oliveira's equation which is given by Equation (3.1) has three variables: height, moment of inertia, and cross section area. It is an equation derived from a study of 11 minarets ranging in height from 23 to 67 meters. During the regression analysis, the properties of the materials used in the minarets, the height of the Spire section, and the height of the boot section were all eliminated [5].

$$f_{\mathrm{Oliveira}} = 38 \times A^{-0.5} \times I^{0.7} \times h^{1.1} \tag{3.1}$$

The equations of Serhatoğlu and Livaoğlu which are given by Equation (3.2) and Equation (3.3) are the results of study on 18 minarets in which two equations were generated, one using both geometric properties and material properties (H, ρ, E, A, I) while the other using only geometric properties (H, A, I). 18 minarets were all smaller than 45m, and it is important to note that most of the minarets have a brick body, thus the modulus of elasticity is low. The height of the minaret is determined by measuring the distance from the beginning of the transitional segment to the end of the body, excluding the height of the Spire section. Additionally, for an unattached minaret, 0.4 times the height of the boot will be added to the height of the minaret. On the other hand, for an attached minaret, 0.33 times the height of the boot will be added to the height of the minaret [6].

$$T_{\text{Serhatoğlu and Livaoğlu 5}} = \frac{2\pi}{32} \frac{h^{1.776} \times A^{1.225} \times \rho^{0.588}}{I^{0.928} \times E^{0.427}} \tag{3.2}$$

$$T_{\text{Serhatoğlu and Livaoğlu 3}} = \frac{2\pi}{3783} \frac{h^{1.398} \times A^{2.329}}{I^{1.478}} \tag{3.3}$$

The equations of Faccio et al [7], Rainieri and Fabbrocino [8], Ministerio de Fomento [9], and Shakya [10], all have a single variable, which is height. The equations of these studies are presented from Equation (3.4) through Equation (3.7).

$$T_{\text{Faccio et al.}} = 0.0187 \times h \tag{3.4}$$

$$T_{\text{Rainieri and Fabbrocino}} = 0.0113 \times h^{1.138} \tag{3.5}$$

$$T_{\text{Ministerio de Fomento}} = 0.05 \times h^{3/4} \tag{3.6}$$

$$f_{\text{Shakya}} = \frac{1}{0.1178 \times h^{0.533}} \tag{3.7}$$

4. METHODOLOGY

4.1 THE MECHANICAL PROPERTIES OF MATERIALS

Determining the mechanical properties of materials that were used in historical minarets is an important topic for researchers. The mechanical properties of materials can be determined in several methods, the compression test method can be applied by taking samples and examining them in the laboratory, or the Schmidt hammer machine can be used to determine the mechanical properties. During this research, the mechanical properties were determined by using the Schmidt hammer test [11]. The stones used in each minaret were examined separately in three different regions, for each region 20 readings were recorded, and the average values were calculated for them as in Table 4.1.

Table 4.1: Schmidt Hammer Test Results.

Minarets	Materials	$N_{Average}$
Minaret of Fatih Mosque	Stone Masonry	38.8
Minaret of Yeni Mosque	Stone Masonry	41.1
Minaret of Nusretiye Mosque	Stone Masonry	46
Minaret of Yeni Valide Mosque	Stone Masonry	41.8
Minaret of Little Hagia Sophia	Stone Masonry (Ottoman Period)	41.8
	Stone Masonry (Republic Period)	40.1
Minaret of Zeynep Sultan Mosque	Stone Masonry	42.46
Minaret of Kepenekçi Sinan Mosque	Stone Masonry	41.88

The mechanical properties of the stones were determined according to relationships provided by [12]. Stone masonry's compressive strength was calculated to be 35% of the stone unit's compressive strength [13]. Based on the Schmidt Hammer rebound number and the previous studies [11], the compressive strength of the brick units that were used in Kepenekçi Sinan Mosque was calculated to be 12.07 MPa while the compressive strength of the brick units that were used in Zeynep Sultan Mosque was calculated to be 15.64 MPa. The historic lime mortar's compressive strength varies between 0.5 MPa and 1.5 MPa. The brick masonry's compressive strength was determined to be 2.78 MPa for Kepenekçi Sinan Mosque and 3.33 MPa for Zeynep Sultan Mosque [14]. Brick masonry's elastic modulus was calculated to be 900 times its compressive strength. Zeynep Sultan Mosque's modulus of elasticity was estimated to be 3000 MPa and Kepenekçi Sinan Mosque's to be 2300 MPa [15]. The tensile strength of the brick masonry is found to be 10% of the compressive strength value of the brick masonry. The properties of the material are presented in Table 4.2.

Table 4.2: Physical and Mechanical Properties of Materials.

Minarets	Materials	E (GPa)	ν	ρ (kg/m^3)	f_{cm} (MPa)	f_c (MPa)	f_t (MPa)
Fatih Mosque	Stone Masonry	10.40	0.30	1911	8.25 – 13.10	29.71	0.83 – 1.31
Yeni Mosque	Stone Masonry	12.42	0.30	1986	9.63 – 15.28	34.66	0.96 – 1.53
Nusretiye Mosque	Stone Masonry	17.59	0.30	2133	13.37 – 21.22	48.13	1.34 – 2.12
Yeni Valide Mosque	Stone Masonry	7.00	0.30	1990	6.10 – 9.63	21.83	0.61 – 0.96
Little Hagia Sophia	Stone Masonry (Ottoman Period)	13.00	0.30	2009	10.09 – 16.02	36.33	1.01 – 1.60
	Stone Masonry (Republic Period)	11.50	0.30	1958	9.00 – 14.30	32.42	0.90 – 1.43
Zeynep Sultan Mosque	Stone Masonry	13.74	0.30	2029	10.55 – 16.75	37.99	1.06 – 1.68
	Brickwork	3.00	0.20	1800	3.33	15.64	0.33
Kepenekçi Sinan Mosque	Stone Masonry	13.17	0.30	2012	10.15 - 16.11	36.55	1.02 - 1.61
	Brickwork	2.50	0.20	1750	2.78	12.07	0.28

f_c: Compressive Strength of Units, f_{cm}: Compressive Strength of Masonry, f_t: Tensile Strength.

4.2 SAP2000 MODELING AND ANALYSIS CONSIDERATIONS

SAP2000 software version 24 was used to examine the seven minarets using the finite element method. The models were created in three dimensions. The seven minarets were developed utilizing macro modeling techniques to reflect how they are. The minarets were designed as solid elements in SAP2000 software program after receiving the architecture plans from the regional director of Istanbul (Figure 4.1). The spiral staircase inside the minaret and the core were taken into consideration from the ground level up to the upper balcony level. The modeling of the balconies and the spire section were taken into consideration, based on the schemes of the minarets. To obtain a model similar to reality, window apertures and door openings were taken into consideration during the modelling. The attached walls around the minaret were also modeled if they existed. The materials applied to the models are shown in Table 4.2. All these parameters have an impact on the stiffness of the minaret and its dynamics response.

4.3 PARAMETERS INFLUENCING VIBRATION PERIOD

During this study, the nonlinear regression analysis for the seven minarets was performed to establish relationships between variables. As a first step, we had to find the variables that will affect the fundamental period, so we used Equation (4.1), which calculates the cantilever's fundamental period and it is considered the closest example of minarets.

$$T = \frac{2\pi}{1.875^2}\sqrt{\frac{\rho\, A\, h^4}{E\, I}} \tag{4.1}$$

As shown in equation (4.1), both geometric variables and material properties variables were used to estimate the fundamental period for the cantilever; therefore, in this study, we used the height, cross-sectional area, moment of inertia, elasticity modulus, and material density as variables to perform the regression analysis. For material properties the values listed in Table 4.2 were used. For geometric properties both the cross-section area and the moment of inertia were calculated at the bottom of the body. Notably, due to the spiral staircase design, only one step exists at each height, the staircase diameter is subtracted from the body diameter when calculating the area and moment of inertia. The height is measured to be the half-height of the boot section adding the height from the bottom of the transitional segment to the top of the spire section without adding the end ornament ($H = 0.5h_1 + h_2 + h_3 + h_4$) (Figure 4.2).

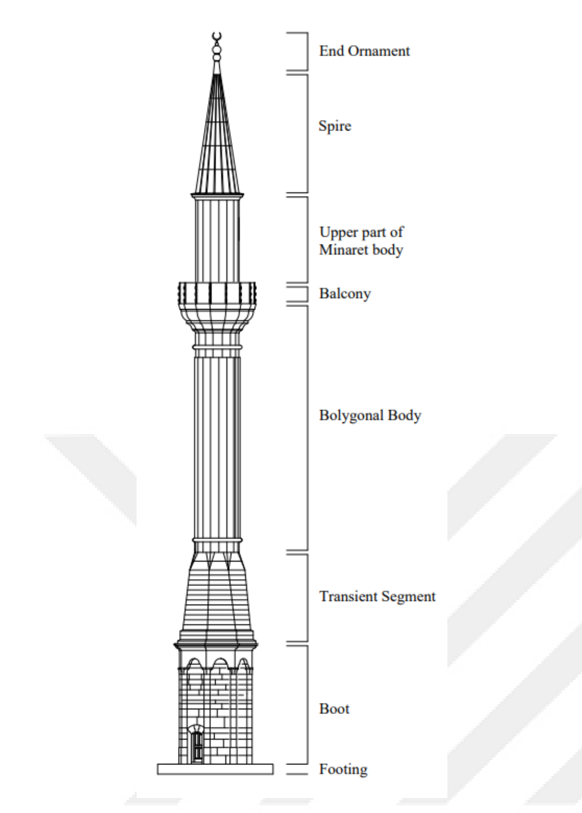

Figure 4.1: Components of Ottoman Minarets.

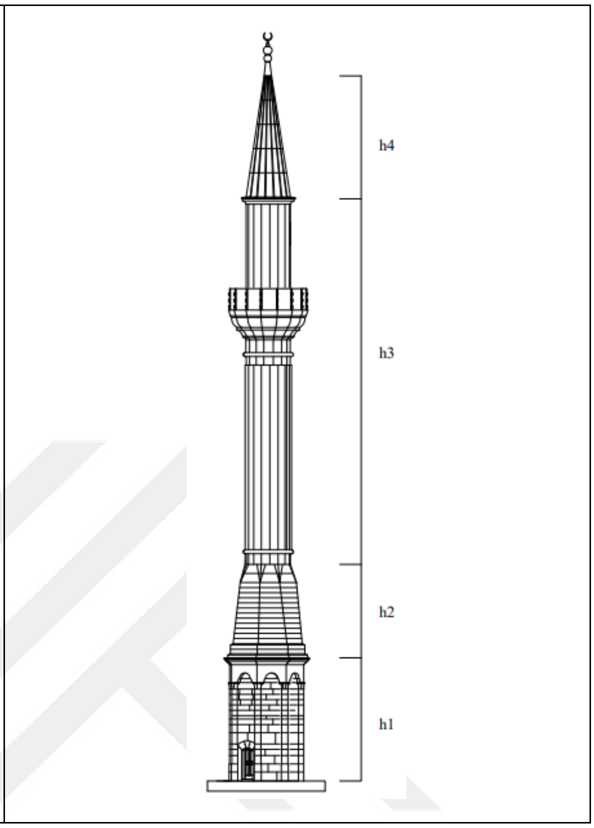

Figure 4.2: H Values During Calculations.

4.4 GROUND MOTIONS CHARACTERISTICS

Following the modeling of the seven minarets in the SAP2000 software program and the determination of the mechanical characteristics of the materials that were used in construction, 9 ground motions were applied to the seven minarets. 6 ground motions caused by earthquakes, 2 ground motions caused by trains, and 1 ground motions caused by vehicles were chosen. Table 4.3 shows all the information about the ground motions that were applied in terms of location, date, time step, number of data points, duration, maximum acceleration of the motion in all directions (N-S, E-W, Z), Approximate Predominant Period in x direction and Approximate Predominant Period in y direction.

Table 4.3: Ground Motion Characteristics.

Name of Ground Motion	Düzce	Düzce	Düzce	Erzincan	Kocaeli	Kocaeli	Train 3A	Train 2C	Vehicle 4B
Location of Recording	Lamont 375	Irigm 496	Bolu	Erzincan	Düzce	Yarimca	Eminönü	Eminönü	Eminönü
Year of Recording	1999	1999	1999	1992	1999	1999	2008	2008	2008
Time Step [sec]	0.010	0.004	0.010	0.005	0.005	0.005	0.002	0.002	0.002
No. of Data Points [N]	4150	7501	5590	3977	5437	7000	10500	10000	11000
Duration [sec]	41.50	30.00	55.90	19.89	27.19	35.00	21.00	20.00	22.00
Maximum Z Acceleration [mm/s^2]	0.192	0.332	0.200	0.235	0.206	0.242	0.360	0.413	0.029
Maximum N-S Acceleration [mm/s^2]	0.890	1.030	0.739	0.387	0.312	0.227	0.516	0.456	0.013
Maximum E-W Acceleration [mm/s^2]	0.514	0.751	0.806	0.496	0.364	0.322	0.346	0.506	0.011
Approximate Predominant Period in x Direction [sec]	0.318	0.227	0.357	0.303	0.278	0.417	0.021	0.018	0.023
Approximate Predominant Period in y Direction [sec]	0.417	0.250	0.318	0.909	0.385	0.556	0.022	0.018	0.023

5. RESULTS

The seven minarets were studied using the SAP2000 program by using the materials that were indicated in Table 4.2. The results are shown in the following sections.

5.1 REGRESSION ANALYSIS

The regression analysis results between each of fundamental period and height, cross sectional area, moment of inertia, modulus of elasticity, and density are shown from the (figure 5.1) to (figure 5.5)

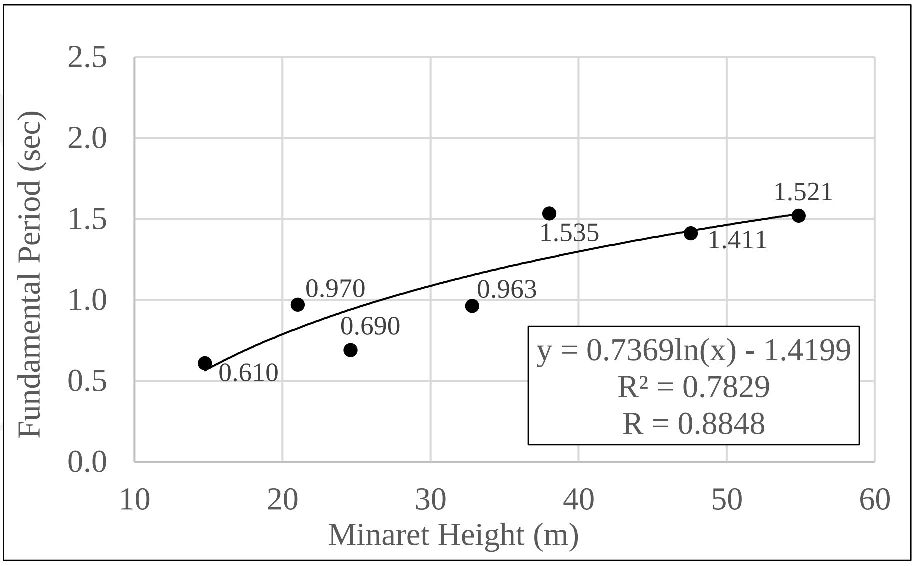

Figure 5.1: Fundamental Period and Height.

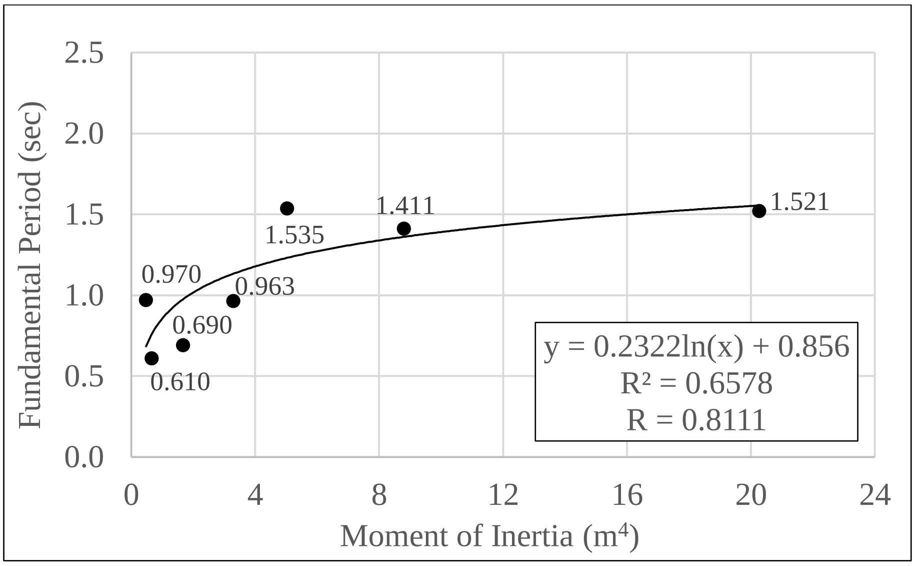

Figure 5.2: Fundamental Period and Moment of Inertia.

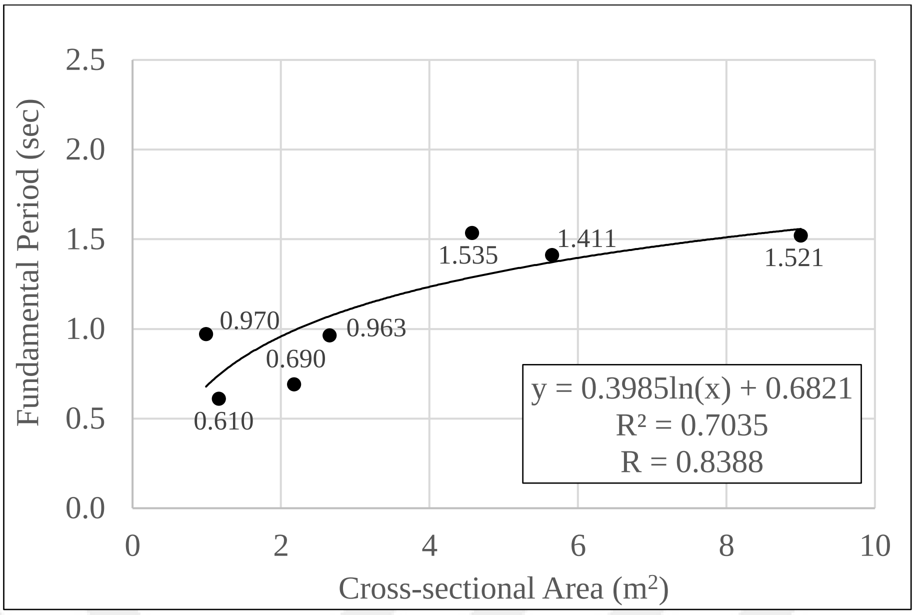

Figure 5.3: Fundamental Period and Cross-Sectional Area.

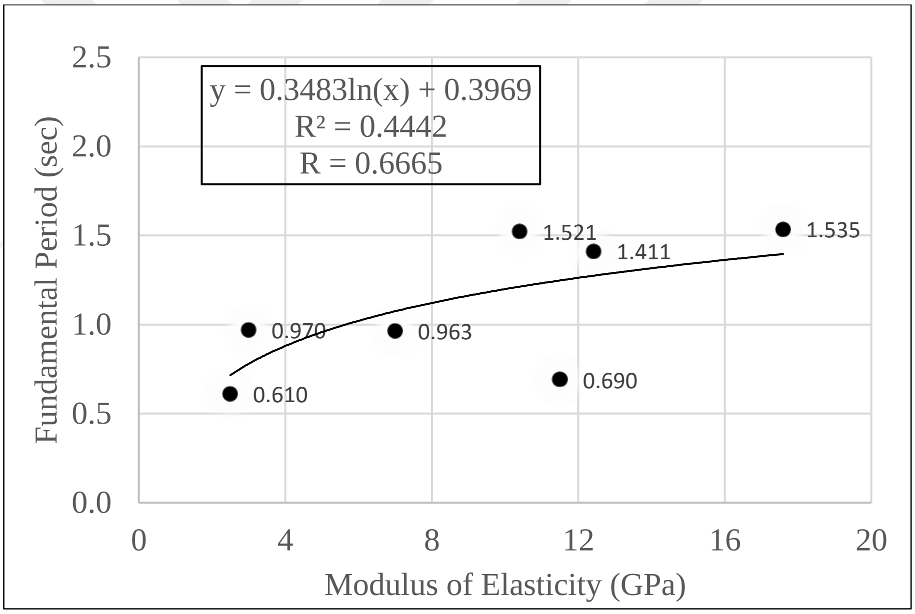

Figure 5.4: Fundamental Period and Modulus of Elasticity.

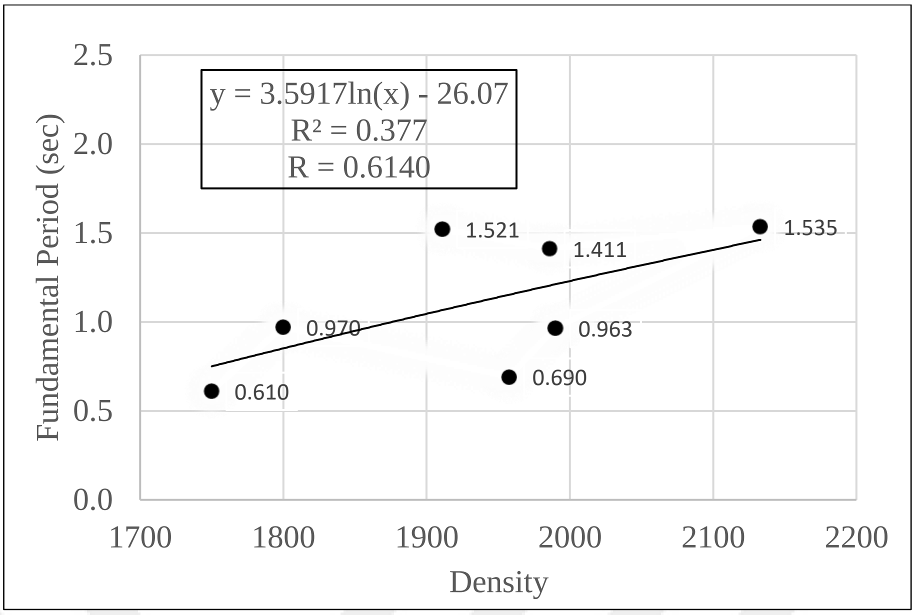

Figure 5.5: Fundamental Period and Density.

Table 5.1 summarizes the regression analysis results, and Table 5.2 shows the regression coefficients of the obtained equations.

Table 5.1: Summary of Regression Analysis Output.

	T_{F5}	T_{F2}
Number of Predictor	5	2
Multiple R	0.999	0.900
R Square	0.999	0.811
Adjusted R^2	0.994	0.716
Standard Error	0.031	0.207
F	186.616	8.572
Significance F	0.055	0.036
Observations	7	7

Table 5.2: Coefficients of Regression Analysis.

	Predictors	Coefficients	Standard Error	t Stat	P-value
T_{F5}	Intercept	-32.502	4.464	-7.282	0.087
	ρ	4.072	0.617	6.604	0.096
	A	2.676	0.206	12.992	0.049
	h	0.836	0.092	9.080	0.070
	E	-0.761	0.076	-10.035	0.063
	I	-1.440	0.112	-12.857	0.049
T_{F2}	Intercept	-2.266	1.739	-1.303	0.262
	h	0.946	0.526	1.799	0.146
	I	-0.072	0.180	-0.399	0.710

According to Table 5.2 the regression analysis produced the following two equations.

$$\mathrm{T_{F5}} = \ln\left(\frac{\rho^{4.072}\mathrm{A}^{2.676}\mathrm{h}^{0.836}}{\mathrm{E}^{0.761}\mathrm{I}^{1.440}}\right) - 32.502 \tag{5.1}$$

$$T_{F2} = ln\left(\frac{h^{0.946}}{I^{0.072}}\right) - 2.266 \tag{5.2}$$

10 different minarets with their own references period have been found from previous studies. Both the previous study's ten minarets and this study's seven minarets were evaluated using the two equations of this study (Equation 5.1 and Equation 5.2), equation of Oliveira, two equations of Serhatoğlu and Livaoğlu, and four different equations (The equations of Faccio et al [7], Rainieri and Fabbrocino [8], Ministerio de Fomento [9], and Shakya [10]) consisting of one variable, which is the height. The results are shown in Table 5.3.

Table 5.3: Comparison of Fundamental Periods of Various Minarets Using Different Suggested Equations.

No	Name and Location of Minarets	Reference	$T_{reference}$	Eqn 5.1	Eqn 5.2	Eqn 3.1	Eqn 3.2	Eqn 3.3	Eqn 3.4	Eqn 3.5	Eqn 3.6	Eqn 3.7
1	İskenderpaşa, Trabzon	[16]	0.78	0.78	0.61	1.08	0.53	0.19	0.38	0.35	0.48	0.59
2	Tabacica, Mostar	[17]	0.54	0.56	0.63	0.66	0.29	0.17	0.43	0.40	0.53	0.63
3	Sultan Ahmed, İstanbul	[18]	1.14	1.07	1.26	0.80	0.50	0.53	0.95	0.99	0.95	0.96
4	Representative, Turkey	[19]	0.90	0.80	0.70	0.68	0.33	0.15	0.47	0.44	0.56	0.66
5	Representative, Turkey	[19]	0.51	0.58	0.46	0.42	0.17	0.09	0.37	0.34	0.47	0.58
6	Typical, Turkey	[20]	1.86	1.58	0.98	1.00	0.78	0.23	0.62	0.60	0.69	0.76
7	Bayburt Grand, Bayburt	[21]	0.70	0.31	0.69	0.42	0.24	0.29	0.54	0.52	0.62	0.71
8	Büyük Mosque, Samsun	[22]	0.98	0.34	0.92	1.05	0.70	0.25	0.60	0.58	0.67	0.75
9	Bitlis Ulu, Bitlis	[23]	0.67	0.13	0.70	0.38	0.30	0.24	0.57	0.55	0.65	0.73
10	Emir Sultan, Bursa	[24]	0.83	1.52	0.75	0.68	0.42	0.32	0.58	0.56	0.65	0.73
11	Fatih, İstanbul	This study	1.52	1.53	1.48	0.72	0.93	0.84	1.32	1.43	1.22	1.14
12	Yeni, İstanbul	This study	1.41	1.38	1.40	0.86	0.83	0.80	1.14	1.22	1.09	1.06
13	Nusretiye, İstanbul	This study	1.54	1.54	1.31	0.77	0.61	0.77	1.08	1.14	1.05	1.02
14	Yeni Valide, İstanbul	This study	0.96	0.96	1.18	0.73	0.53	0.34	0.87	0.90	0.89	0.91
15	Little Hagia Sophia, İstanbul	This study	0.69	0.69	0.92	0.79	0.39	0.40	0.62	0.61	0.69	0.76
16	Zeynep Sultan, İstanbul	This study	0.97	0.97	0.90	1.15	0.61	0.33	0.53	0.51	0.61	0.70
17	Kepenekçi Sinan, İstanbul	This study	0.61	0.60	0.49	0.69	0.31	0.18	0.35	0.31	0.45	0.56

5.2 MODAL ANALYSIS

The results of modal analysis are shown in Table 5.4.

Table 5.4: Results of Modal Analysis.

Minarets	Modes	f (Hz)	T (s)	Modal Participating Mass Ratio (MPMR) (%)					
				U_X	U_Y	U_Z	R_X	R_Y	R_Z
Fatih Mosque	1	0.66	1.52	11.88	8.58	0.00	29.04	38.85	2.34
	2	0.67	1.49	8.81	10.99	0.00	38.27	29.40	1.07
	3	2.96	0.34	13.82	0.96	0.04	0.05	0.47	0.23
	4	3.06	0.33	1.13	9.13	0.01	1.07	0.07	1.36
	5	6.13	0.16	28.15	0.50	0.29	0.06	2.72	0.14
	6	6.91	0.14	0.01	0.91	0.02	0.00	0.04	45.85
Yeni Mosque	1	0.71	1.41	5.10	13.38	0.00	50.37	18.95	2.77
	2	0.72	1.39	13.61	4.92	0.00	18.72	50.95	0.43
	3	3.39	0.30	4.34	4.39	0.01	0.75	0.50	0.69
	4	3.48	0.29	5.49	3.40	0.01	0.64	0.65	0.47
	5	7.75	0.13	20.16	0.19	0.35	0.00	0.51	0.63
	6	8.26	0.12	0.51	8.82	0.00	0.01	0.02	3.03
Nusretiye Mosque	1	0.65	1.54	5.85	10.50	0.00	45.54	25.08	0.00
	2	0.66	1.51	10.15	5.51	0.00	25.00	45.51	0.00
	3	3.15	0.32	2.49	6.86	0.00	1.47	0.37	0.00
	4	3.29	0.30	5.73	1.39	0.00	0.59	1.63	0.00
	5	6.98	0.14	9.40	11.91	0.00	0.09	0.11	0.00
	6	7.85	0.13	6.70	3.95	0.00	0.03	0.01	0.08
Yeni Valide Mosque	1	1.04	0.96	24.08	1.82	0.00	4.49	60.53	4.17
	2	1.17	0.85	1.49	18.84	0.00	59.57	4.58	0.05
	3	3.65	0.27	20.28	0.90	0.00	0.00	0.01	1.00
	4	4.55	0.22	0.66	11.26	0.02	1.61	0.07	0.22
	5	7.17	0.14	18.78	0.37	0.03	0.11	4.20	1.63
	6	8.63	0.12	0.33	1.64	0.01	0.09	0.20	26.48

Table 5.4: Results of Modal Analysis "Tables Continued".

Little hagia Sophia Mosque	1	1.43	0.69	27.96	14.71	0.00	18.62	35.45	0.00
	2	1.45	0.69	14.55	27.75	0.00	35.58	18.71	0.00
	3	6.99	0.14	20.34	0.97	0.00	0.20	3.46	0.00
	4	7.07	0.14	0.87	20.52	0.00	3.45	0.12	0.01
	5	14.07	0.07	0.05	0.00	0.00	0.00	0.03	48.89
	6	15.25	0.07	10.38	1.07	0.00	0.63	6.46	0.07
Zeynep Sultan Mosque	1	1.03	0.97	0.00	15.22	0.00	70.85	0.00	0.52
	2	1.04	0.96	15.12	0.00	0.00	0.00	72.39	0.00
	3	6.19	0.16	1.71	2.48	0.00	1.23	0.90	0.10
	4	6.34	0.16	2.44	1.81	0.00	0.88	1.31	0.04
	5	9.62	0.10	0.00	0.00	0.00	0.00	0.00	3.24
	6	14.57	0.07	1.20	1.42	0.00	0.20	0.19	0.07
Kepenekçi Sinan Mosque	1	1.64	0.61	13.71	0.57	0.00	2.61	68.12	0.76
	2	1.65	0.60	0.57	13.38	0.00	60.73	2.92	0.74
	3	9.69	0.10	5.46	0.02	0.00	0.00	1.59	0.22
	4	9.73	0.10	0.01	4.01	0.00	1.56	0.01	0.06
	5	11.00	0.09	0.06	0.00	0.01	0.00	0.00	3.40
	6	21.19	0.05	2.68	3.89	1.55	0.03	0.04	1.78

5.3 SELF-WEIGHT ANALYSIS

The seven minarets were analyzed under the effect of self-weight, Table 5.5 presents the results of self-weight and vertical stresses for each minaret.

Table 5.5: Results of Self-Weight Analysis.

Minarets	Self-Weight (kN)	Vertical stresses (MPa)			
		At the Base of Spire	At the Top and at the Base of Cylinder Body	At the Top and at the Base of Transitional Segment	At the Top and at the Base of Boot
Fatih Mosque	19928	0.07	0.07 – 1.00	1.00 – 0.63	0.63 – 1.46
Yeni Mosque	11160	0.06	0.06 – 1.00	1.00 – 0.3	0.30 – 1.45
Nusretiye Mosque	5768	0.08	0.08 – 0.90	0.90 – 0.90	0.90 – 1.84
Yeni Valide Mosque	3725	0.07	0.07 – 0.50	0.50 – 0.25	0.25 – 0.75
Little Hagia Sophia	1870	0.04	0.04 – 0.45	0.45 – 0.20	0.20 – 1.14
Zeynep Sultan Mosque	1700	0.04	0.04 – 0.42	0.42 – 0.07	0.07 – 1.61
Kepenekçi Sinan Mosque	1146	0.02	0.02 – 0.26	0.26 – 0.07	0.07 – 1.22

The vertical stresses along the height of each minaret and the corresponding deformed shape of each minaret are presented from (Figure 5.6) to (Figure 5.12).

a. Minaret of Fatih Mosque

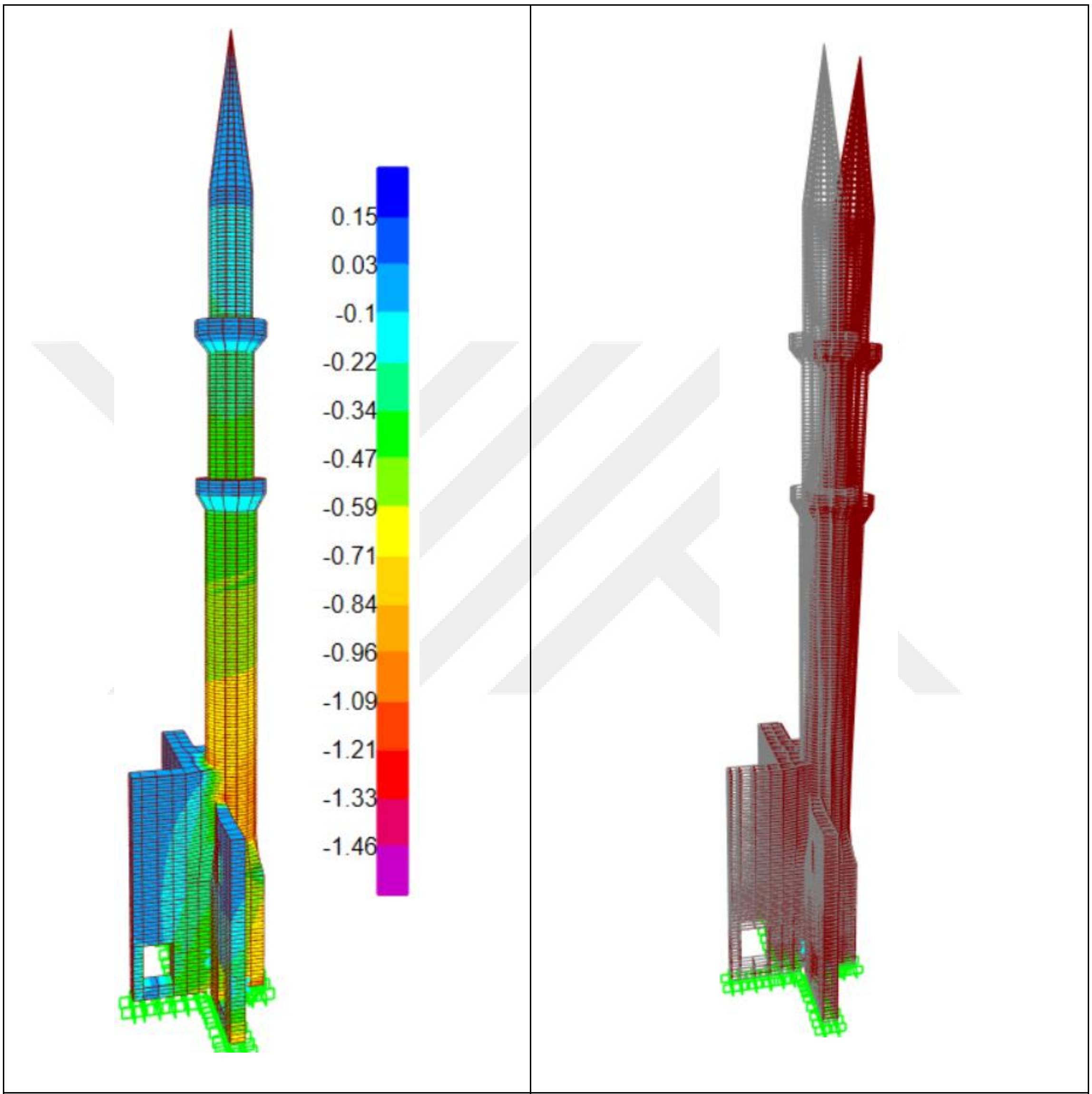

Vertical stresses (MPa)	Deformed shape

Figure 5.6: Vertical Stresses and Deformed Shape for the Minaret of Fatih Mosque.

b. Minaret of Yeni Mosque

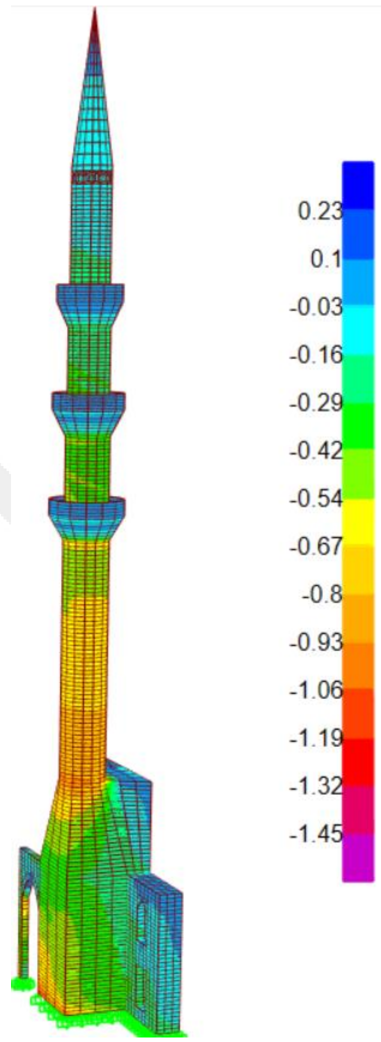	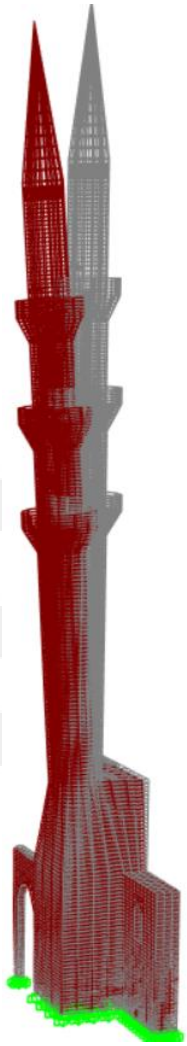
Vertical stresses (MPa)	Deformed shape

Figure 5.7: Vertical Stresses and Deformed Shape for the Minaret of Yeni Mosque.

c. Minaret of Nusretiye Mosque

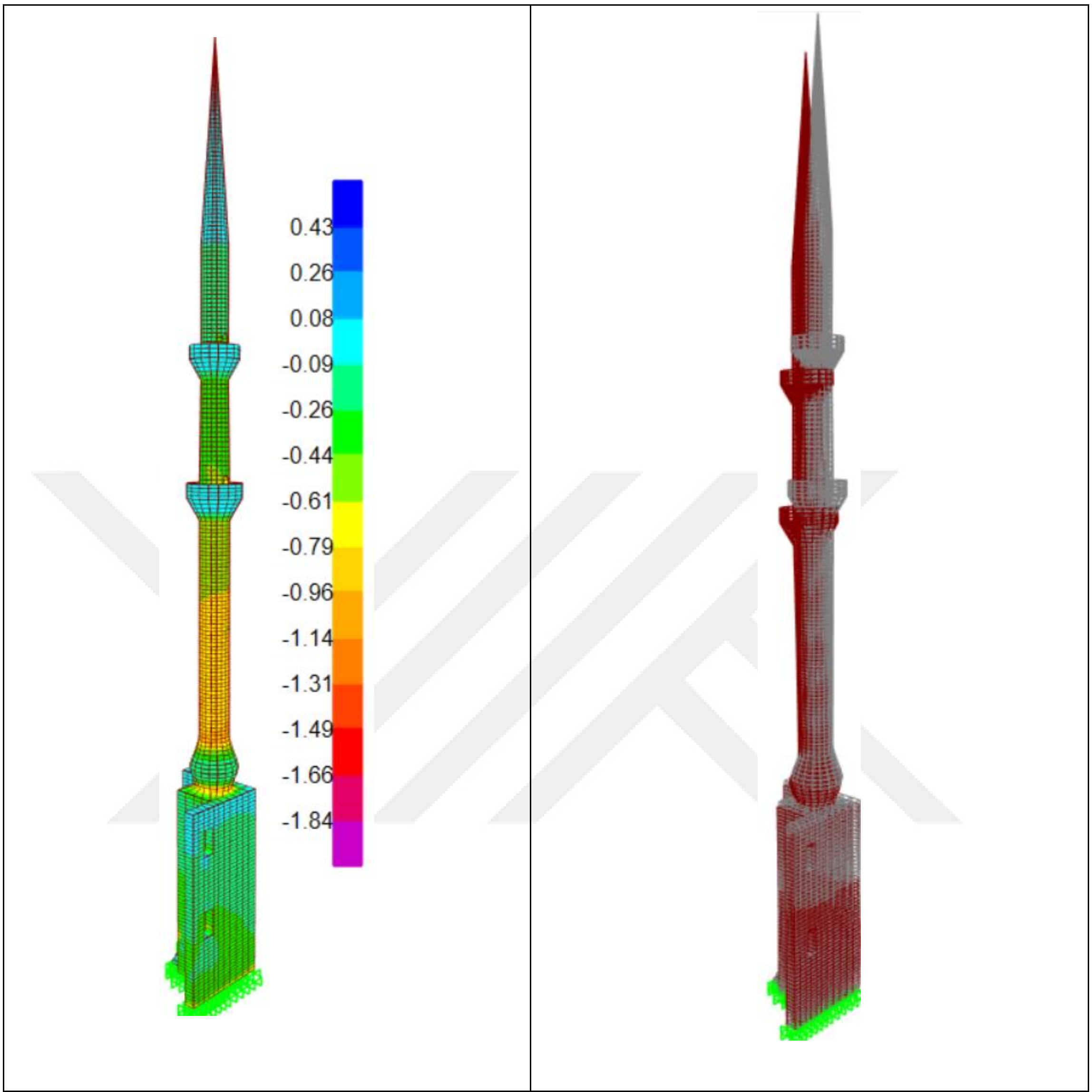

Vertical stresses (MPa)	Deformed shape

Figure 5.8: Vertical Stresses and Deformed Shape for the Minaret of Nusretiye Mosque.

d. Minaret of Yeni Valide Mosque

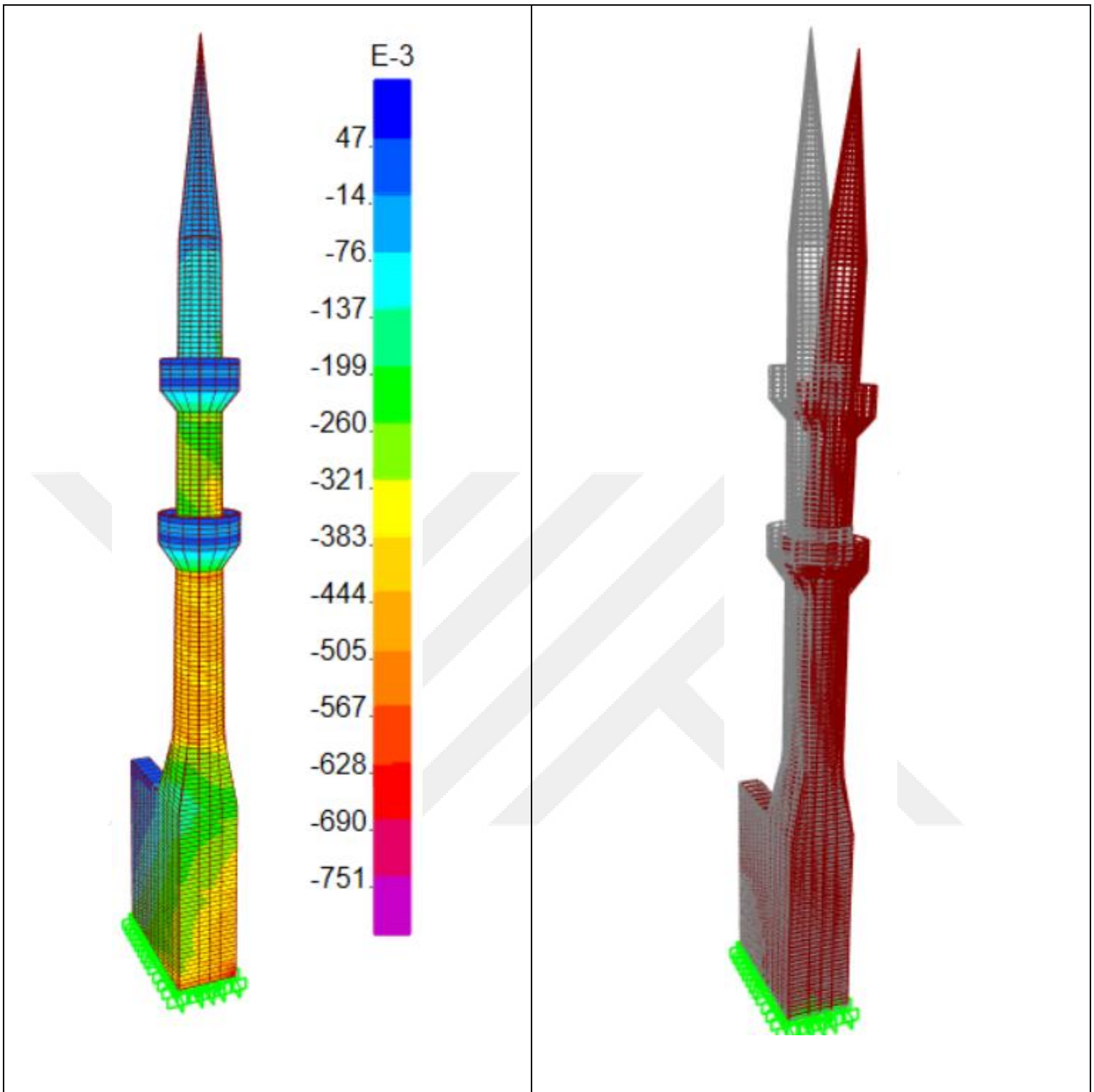

Vertical stresses (MPa)	Deformed shape

Figure 5.9: Vertical Stresses and Deformed Shape for the Minaret of Yeni Valide Mosque.

e. Minaret of Little Hagia Sophia Mosque

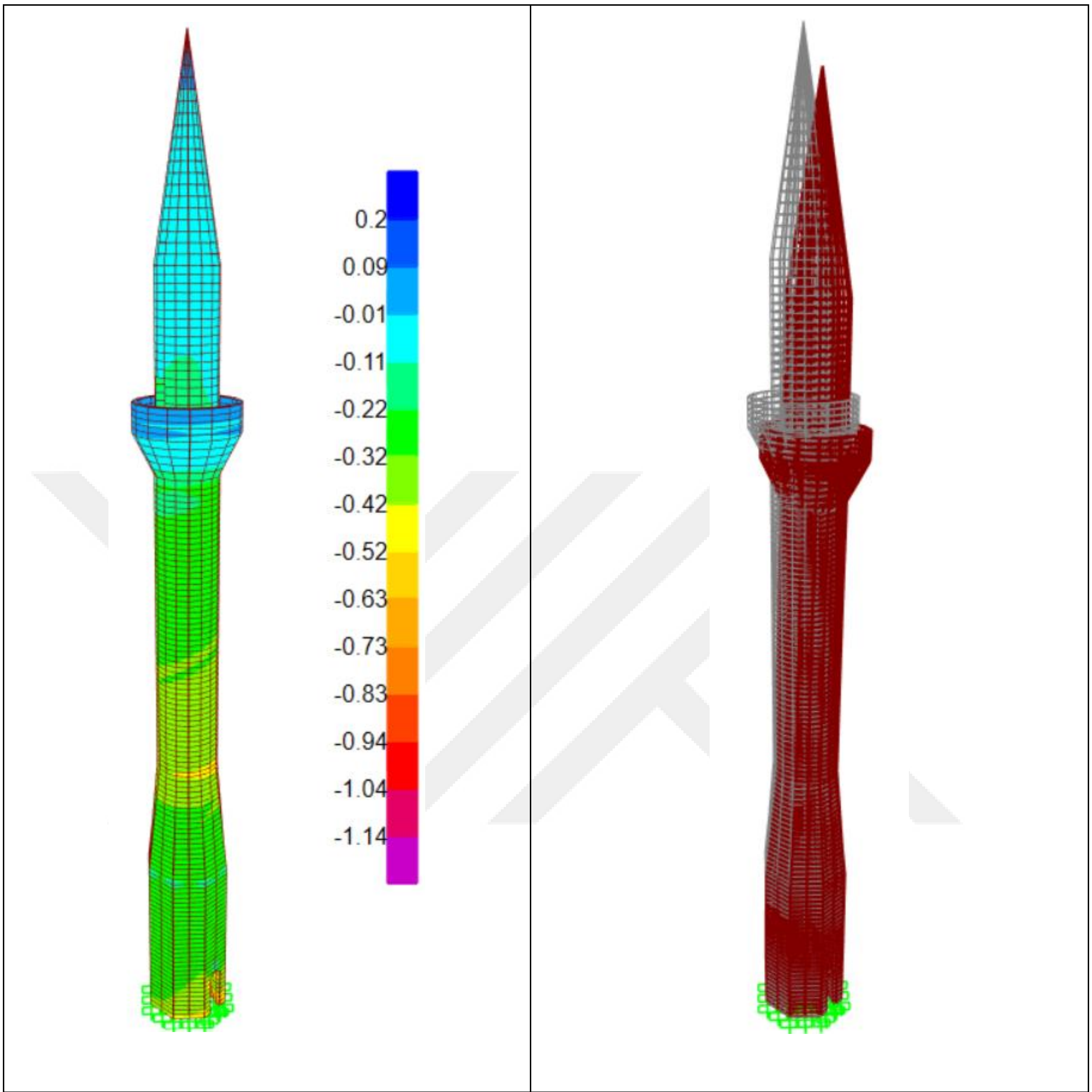

Vertical stresses (MPa)	Deformed shape

Figure 5.10: Vertical Stresses and Deformed Shape for the Minaret of Little Hagia Sophia Mosque.

f. Minaret of Zeynep Sultan Mosque

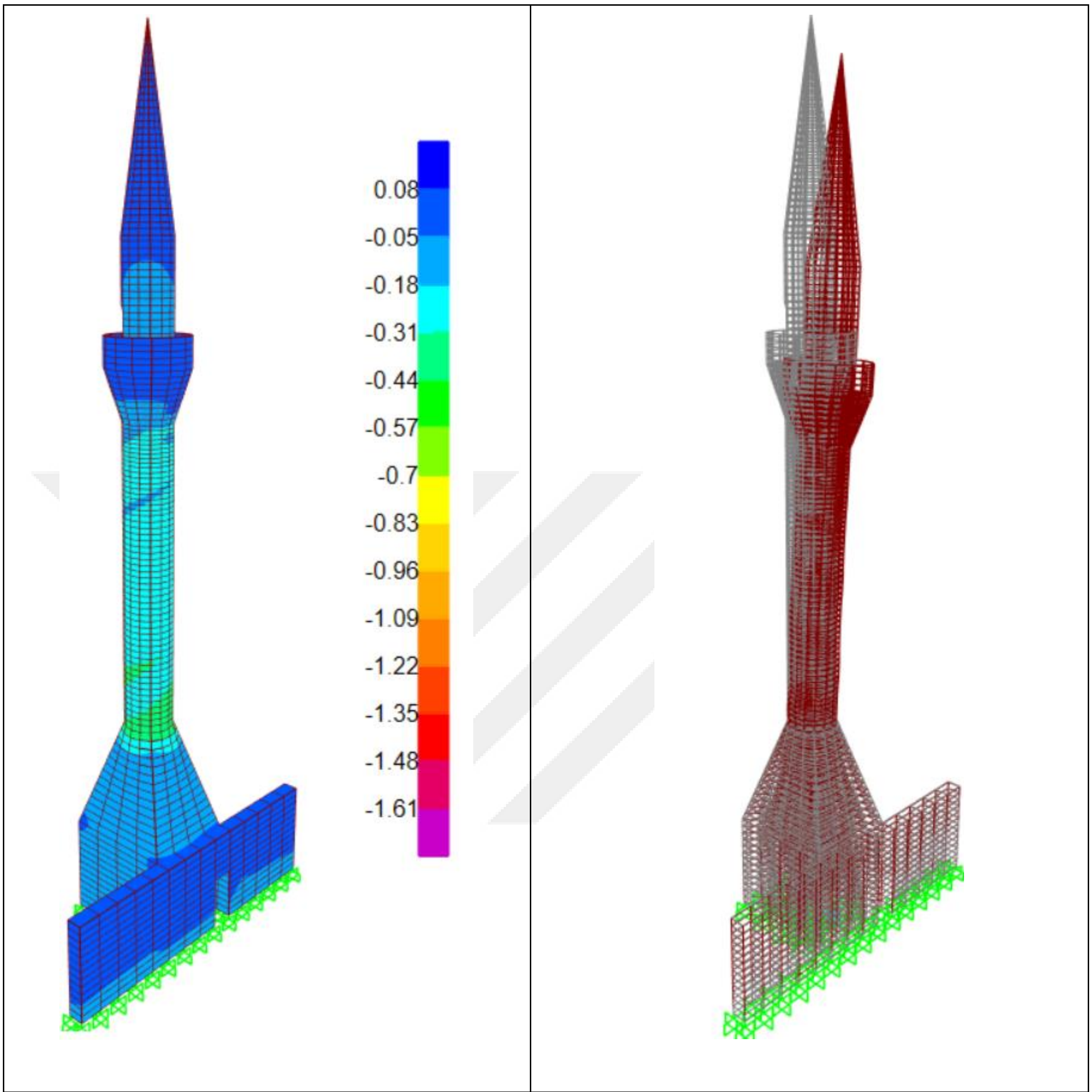

Vertical stresses (MPa)	Deformed shape

Figure 5.11: Vertical Stresses and Deformed Shape for the Minaret of Zeynep Sultan Mosque.

g. Minaret of Kepenekçi Sinan Mosque

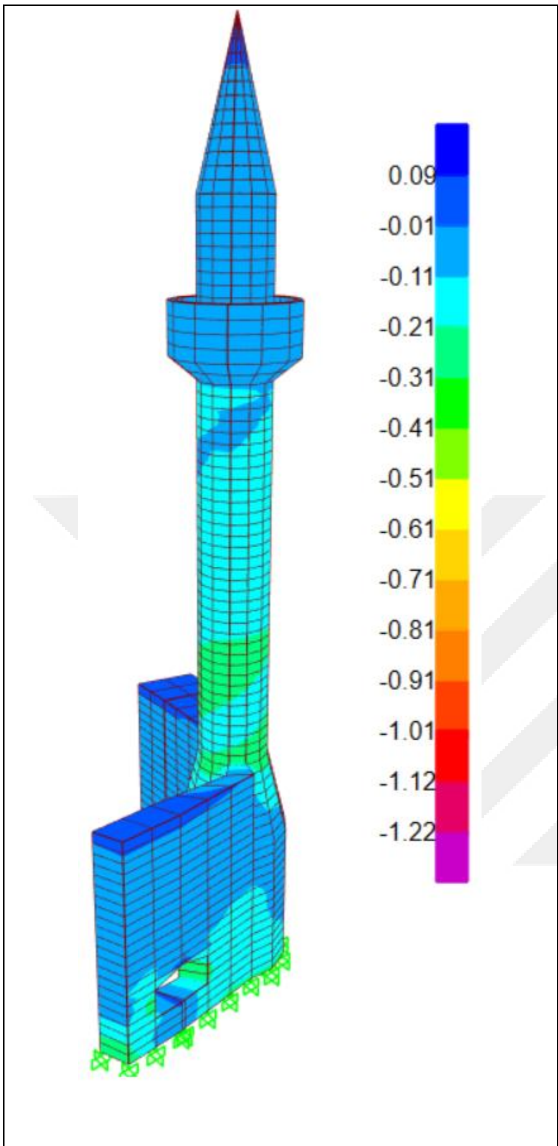

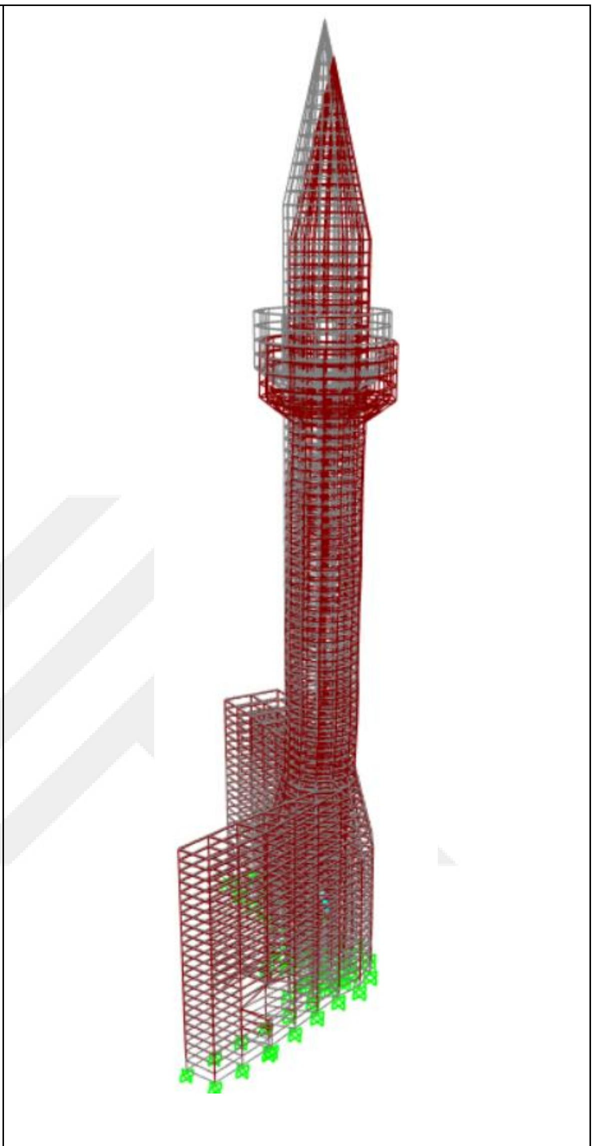

Vertical stresses (MPa)	Deformed shape

Figure 5.12: Vertical Stresses and Deformed Shape for the Minaret of Kepenekçi Sinan Mosque.

5.4 TIME HISTORY ANALYSIS

Through (figure 5.13) to (figure 5.30) response spectrum curves are displayed in both the x and y directions, incorporating a 5% damping ratio.

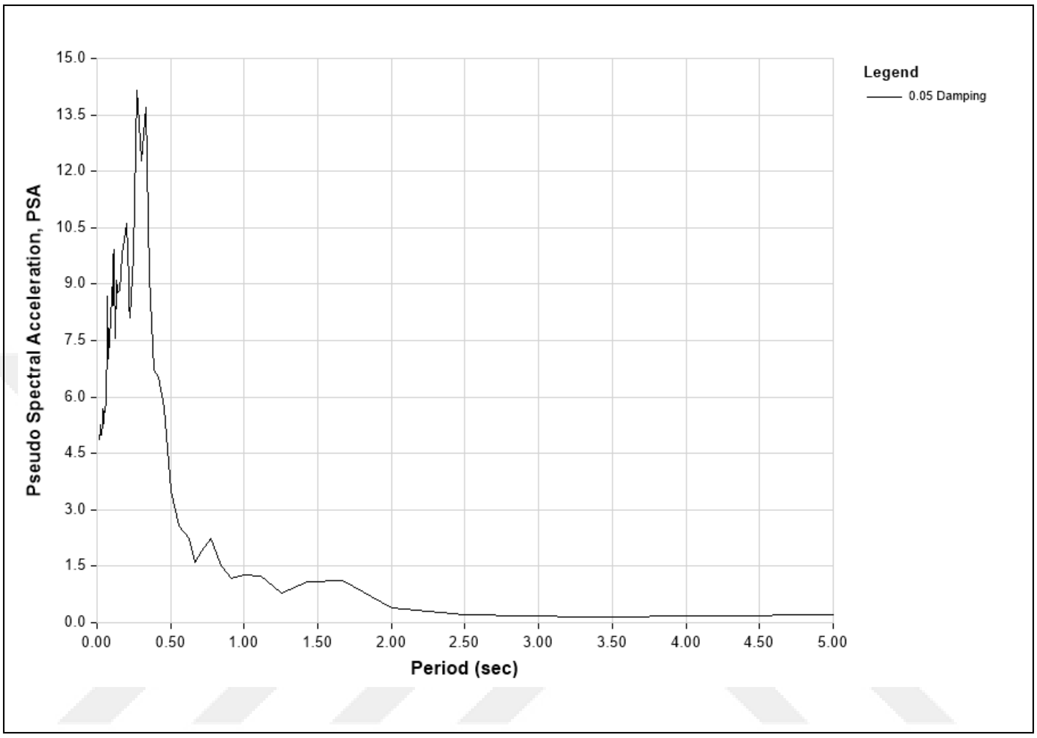

Figure 5.13: Düzce Earthquake at Lamont 375 in X-Direction.

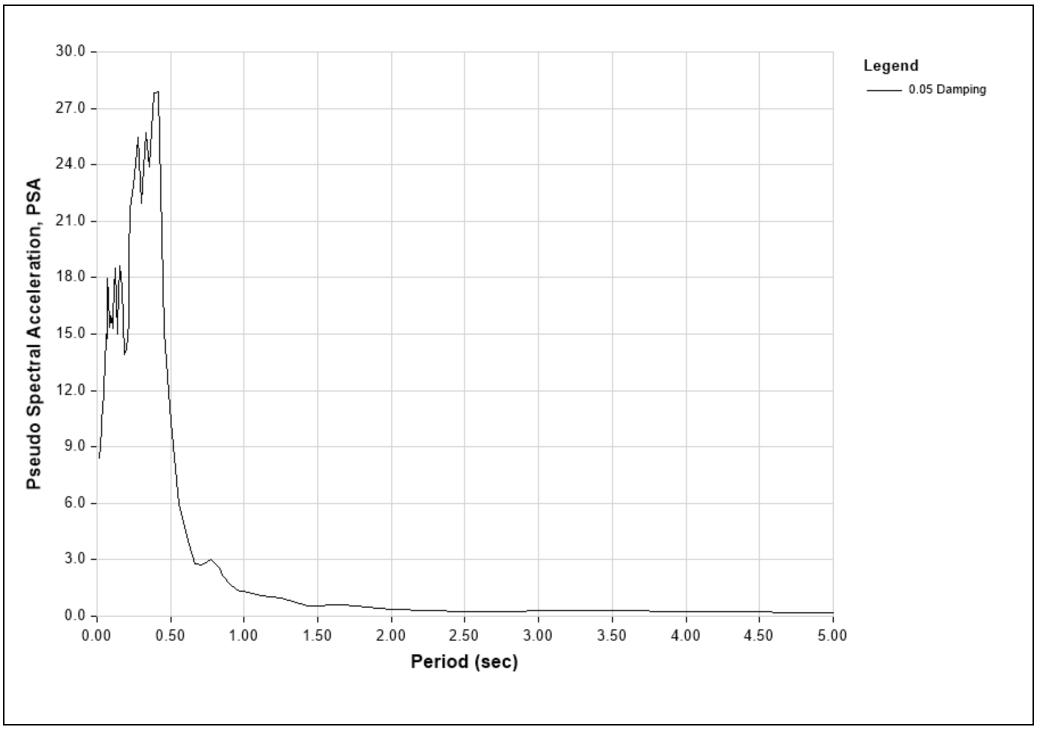

Figure 5.14: Düzce Earthquake at Lamont 375 in Y-Direction.

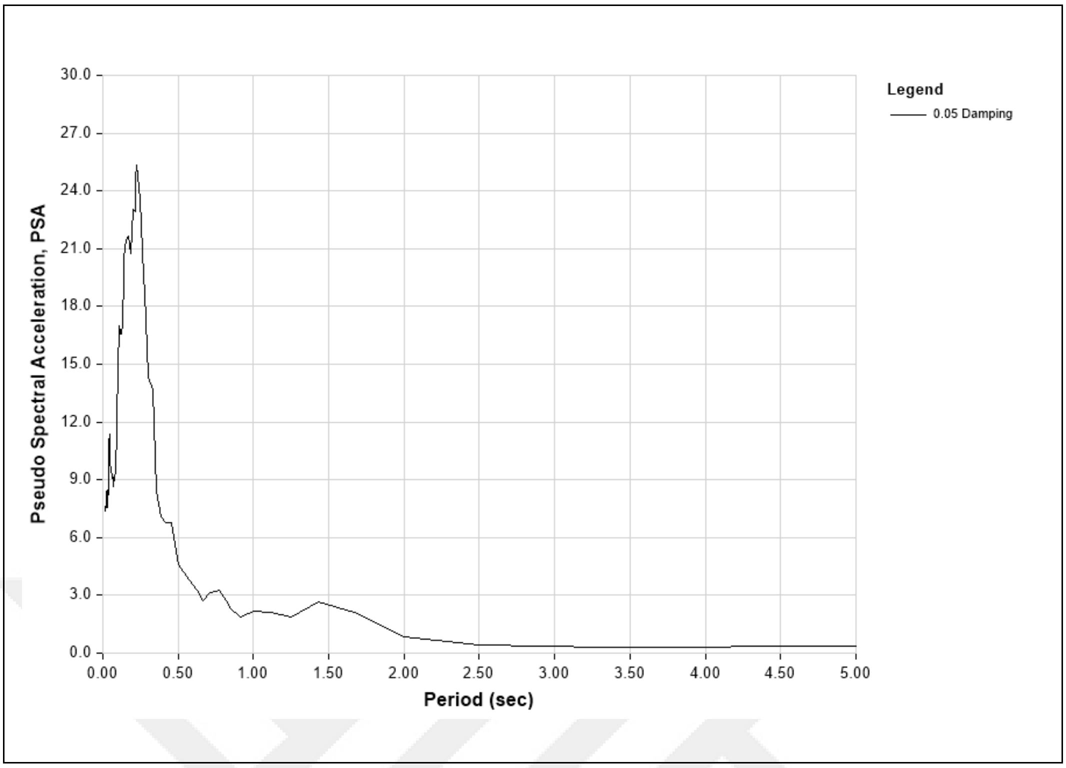

Figure 5.15: Düzce Earthquake at Irigm 496 in X-Direction.

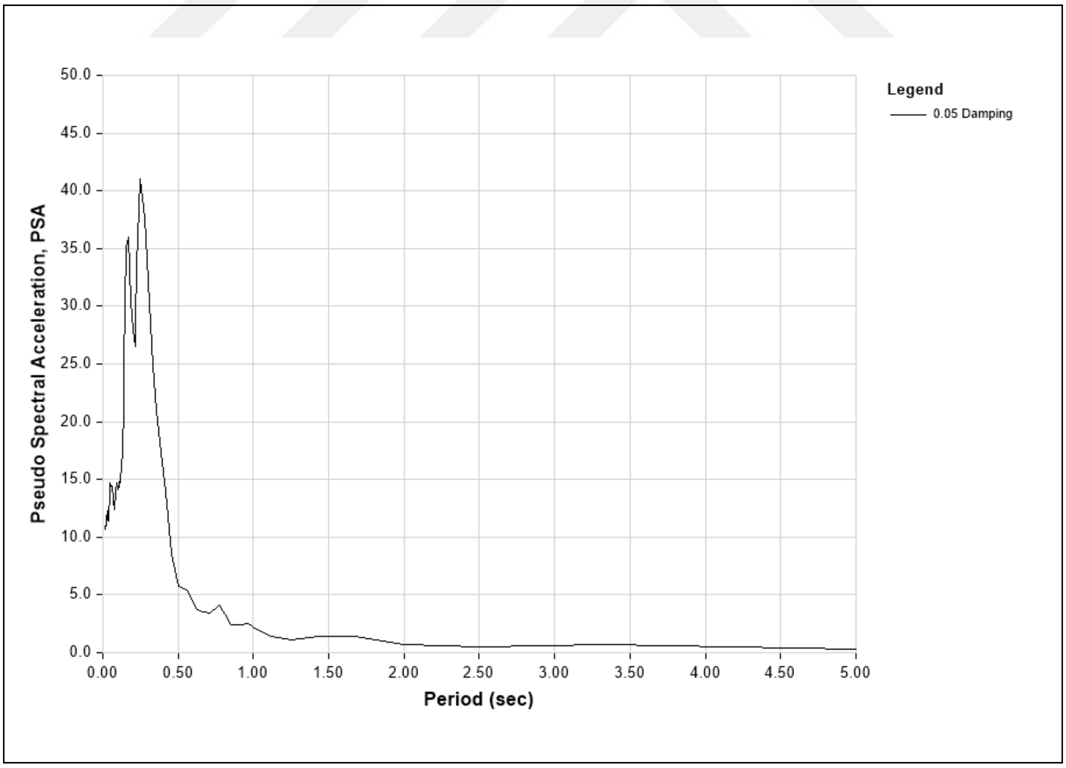

Figure 5.16: Düzce Earthquake at Irigm 496 in Y-Direction.

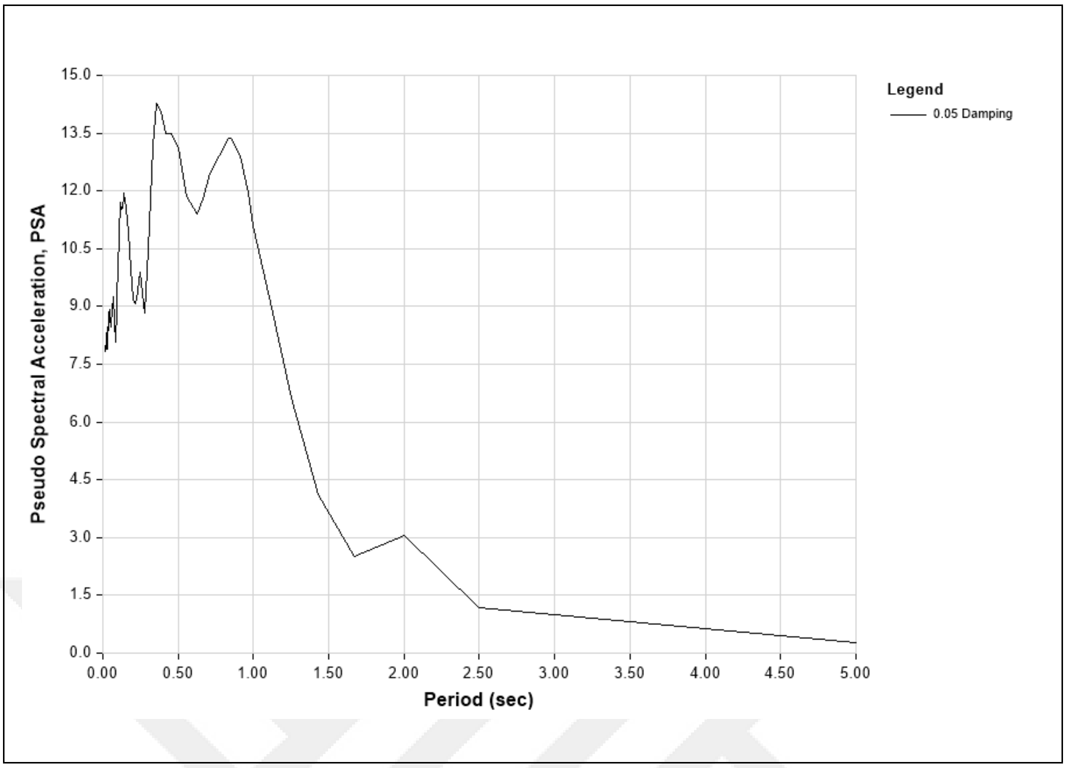

Figure 5.17: Düzce Earthquake at Bolu in X-Direction.

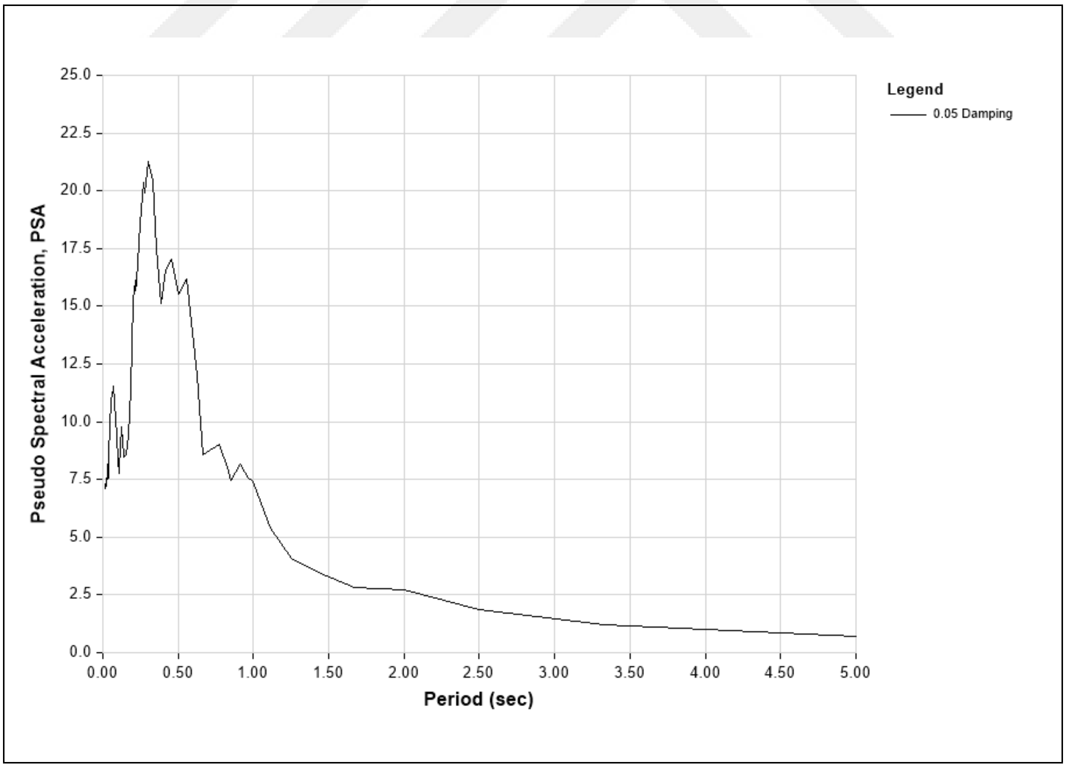

Figure 5.18: Düzce Earthquake at Bolu in Y-Direction.

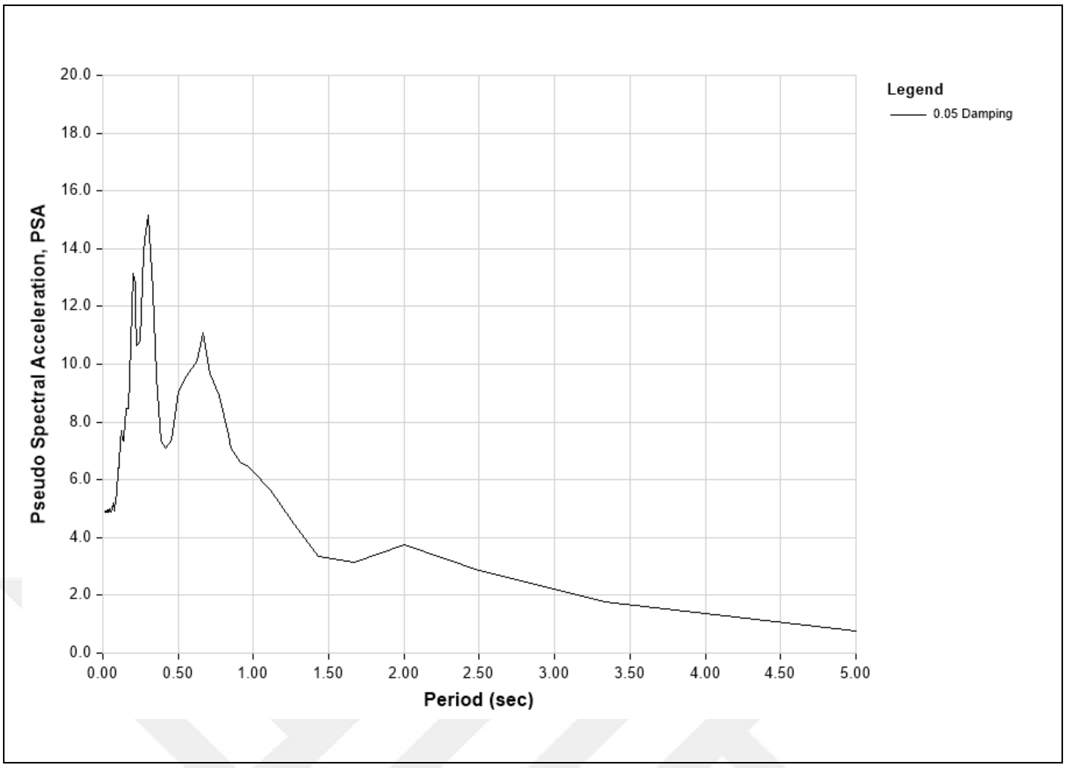

Figure 5.19: Erzincan Earthquake at Erzincan in X-Direction.

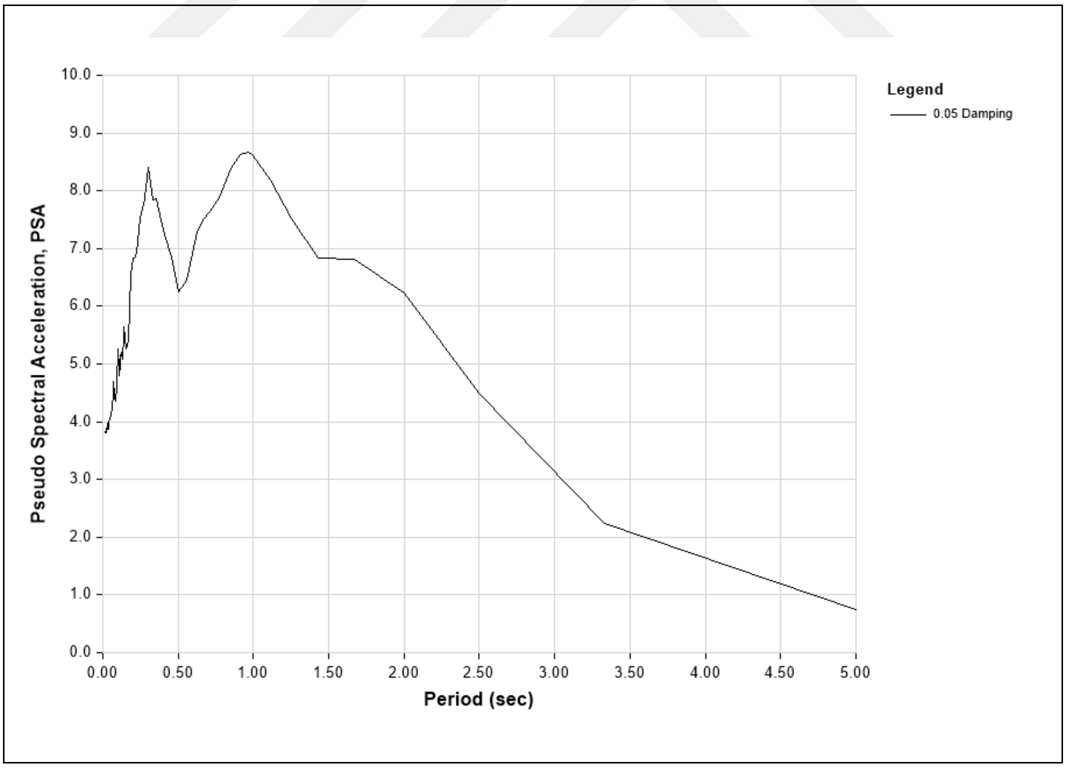

Figure 5.20: Erzincan Earthquake at Erzincan in Y-Direction.

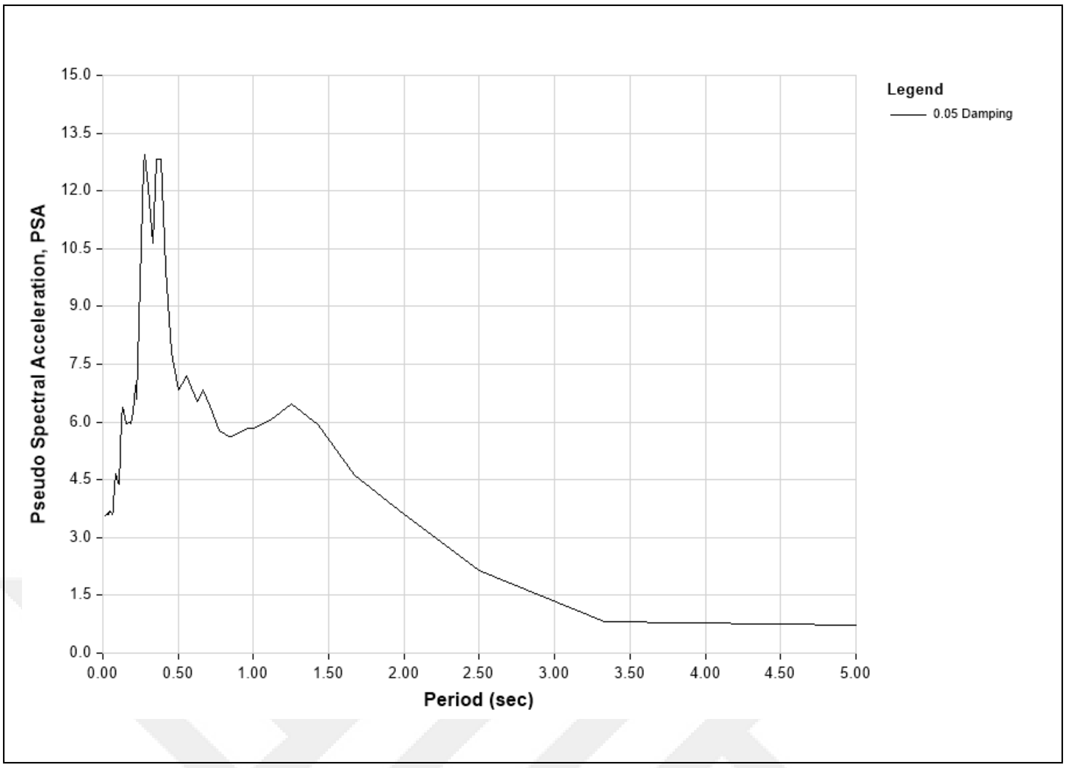

Figure 5.21: Kocaeli Earthquake at Düzce in X-Direction.

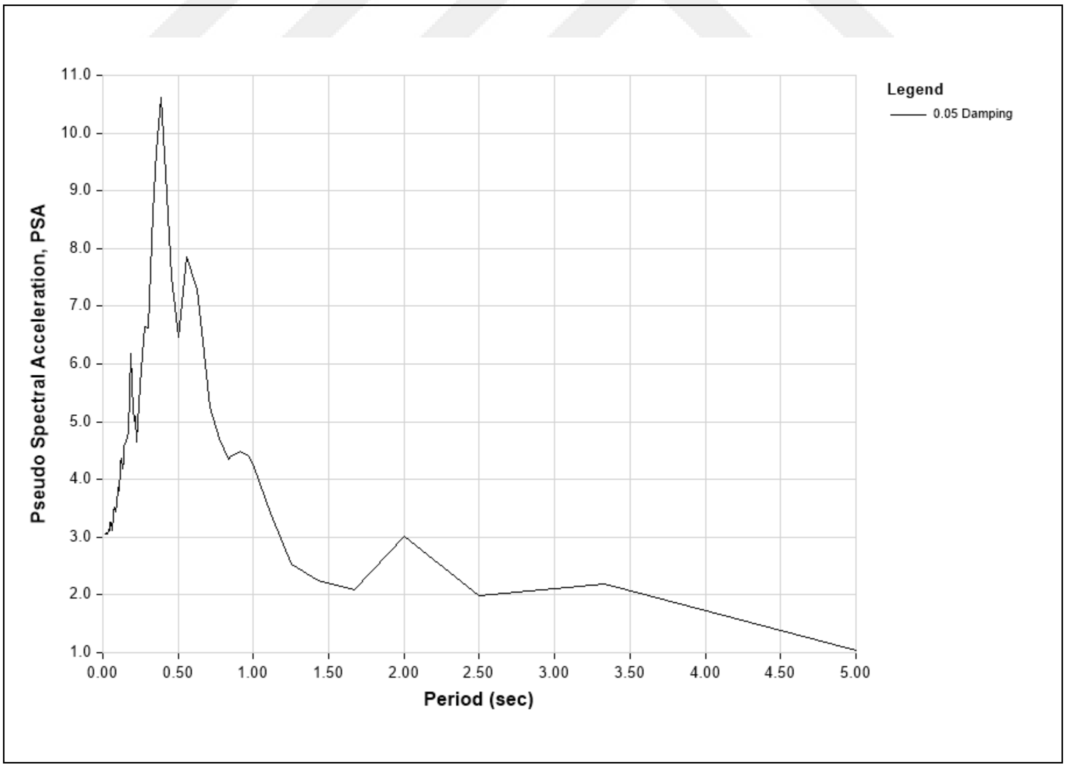

Figure 5.22: Kocaeli Earthquake at Düzce in Y-Direction.

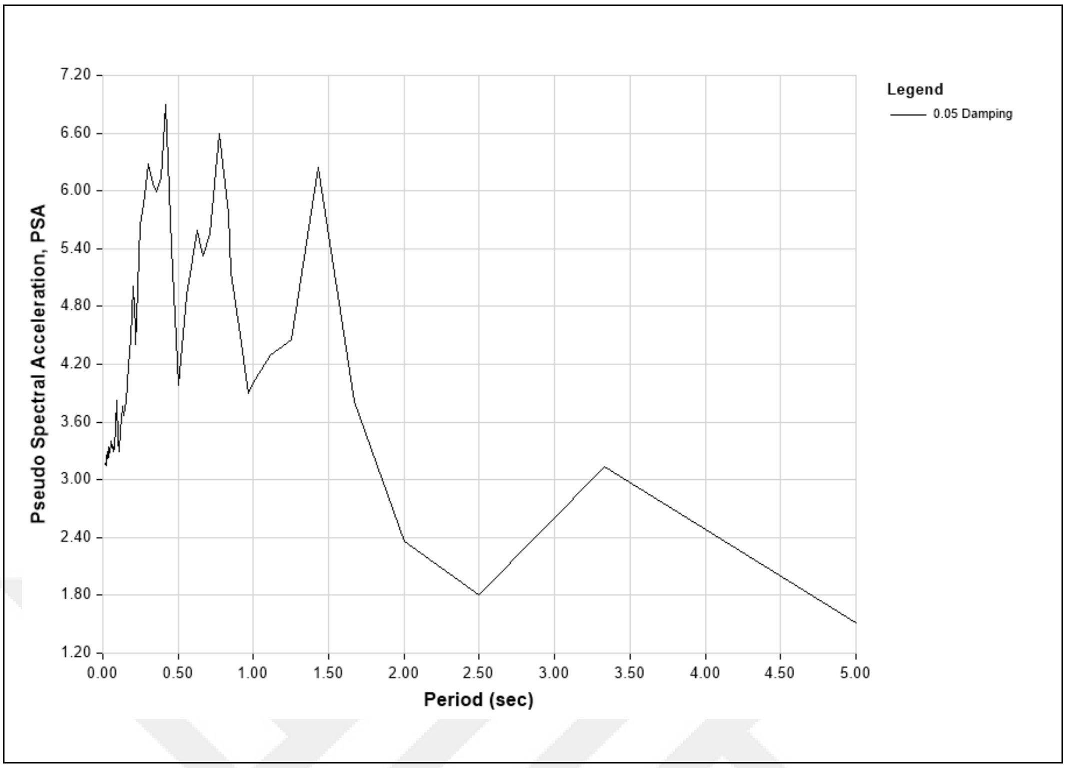

Figure 5.23: Kocaeli Earthquake at Yarimca in X-Direction.

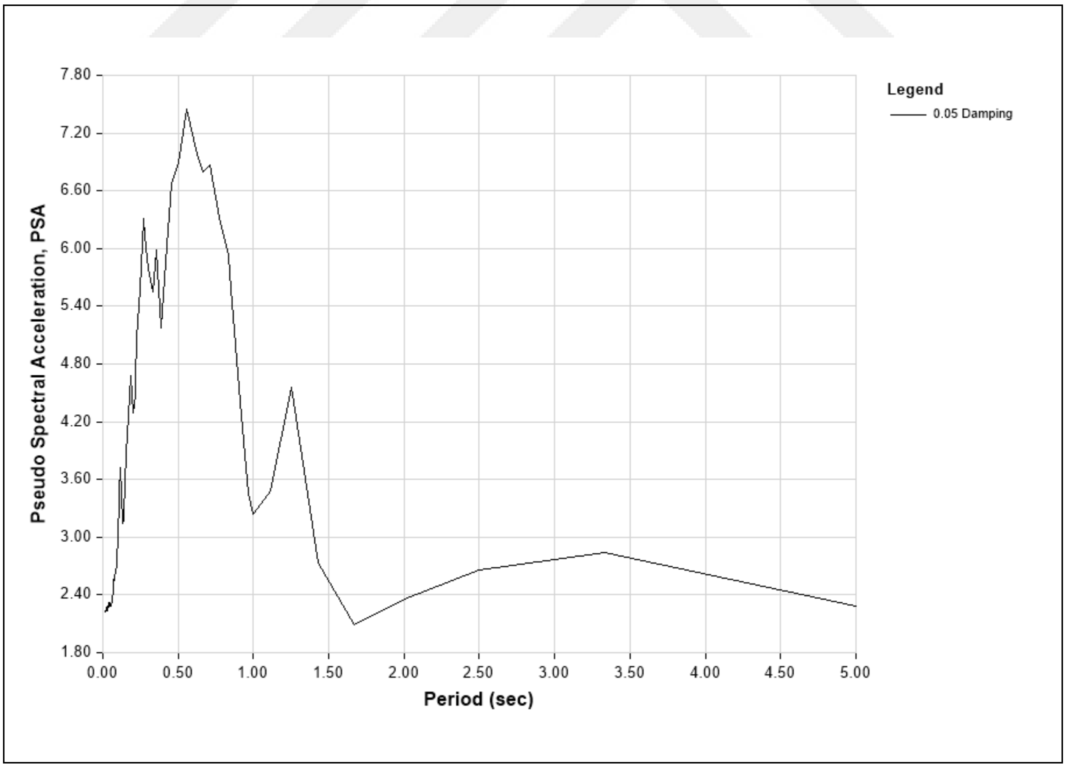

Figure 5.24: Kocaeli Earthquake at Yarimca in Y-Direction.

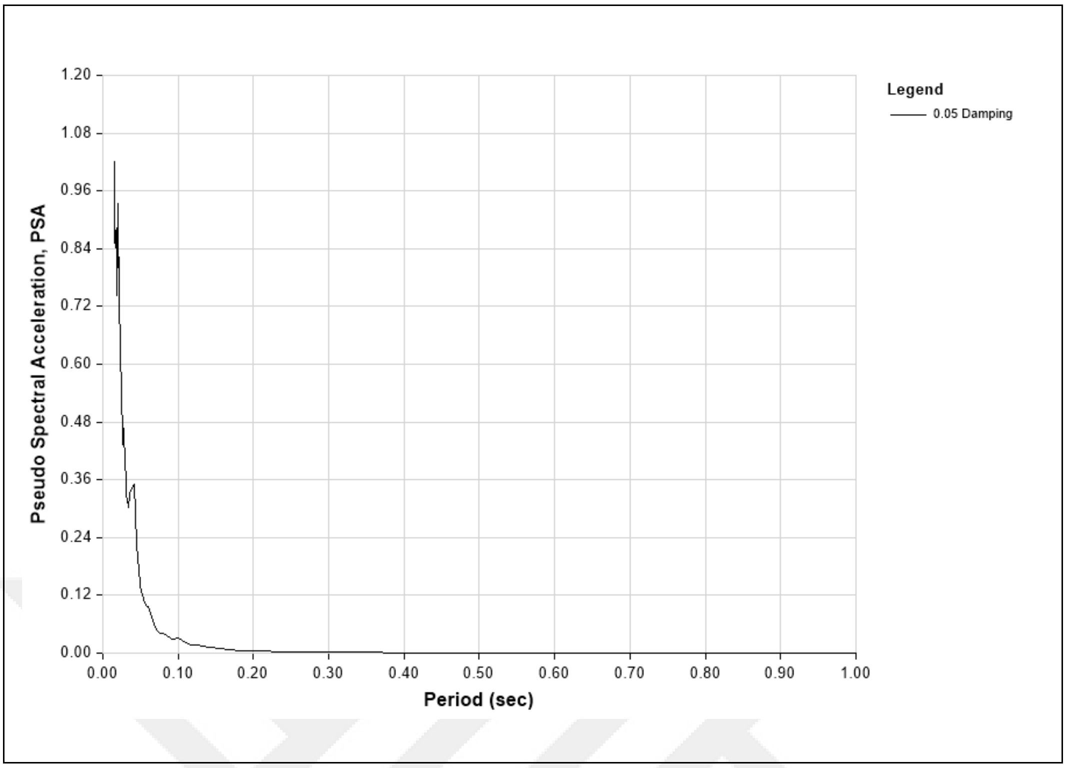

Figure 5.25: Train 3A in X-Direction.

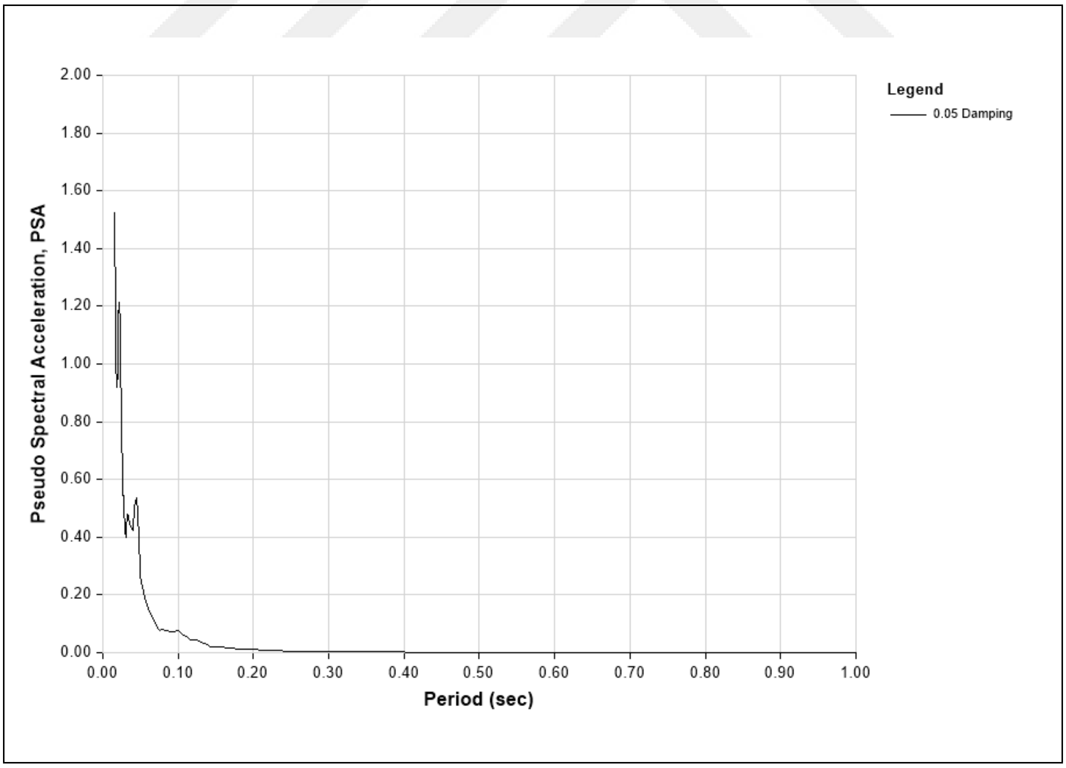

Figure 5.26: Train 3A in Y-Direction.

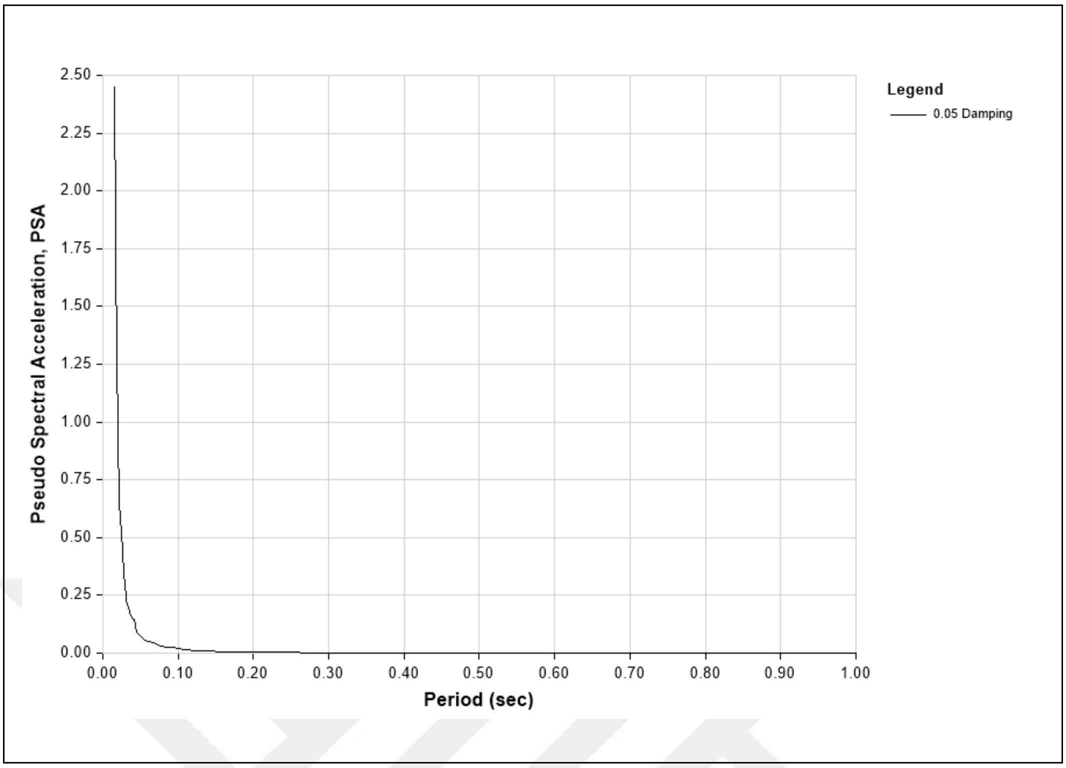

Figure 5.27: Train 2C in X-Direction.

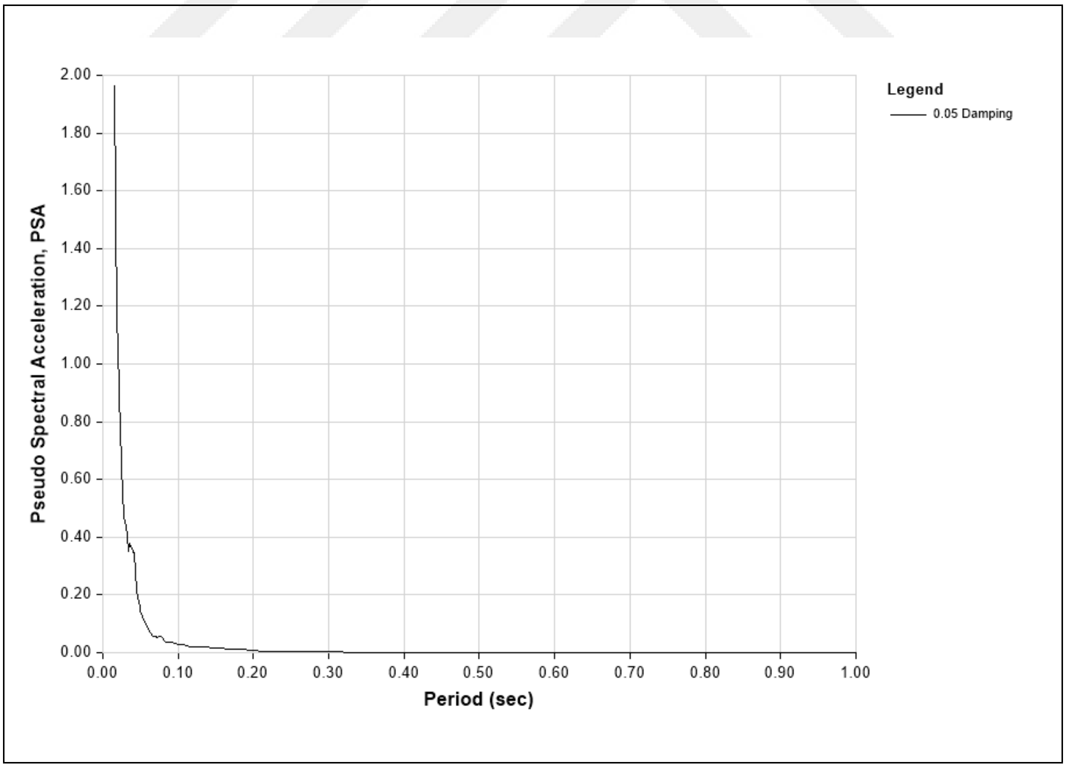

Figure 5.28: Train 2C in Y-Direction.

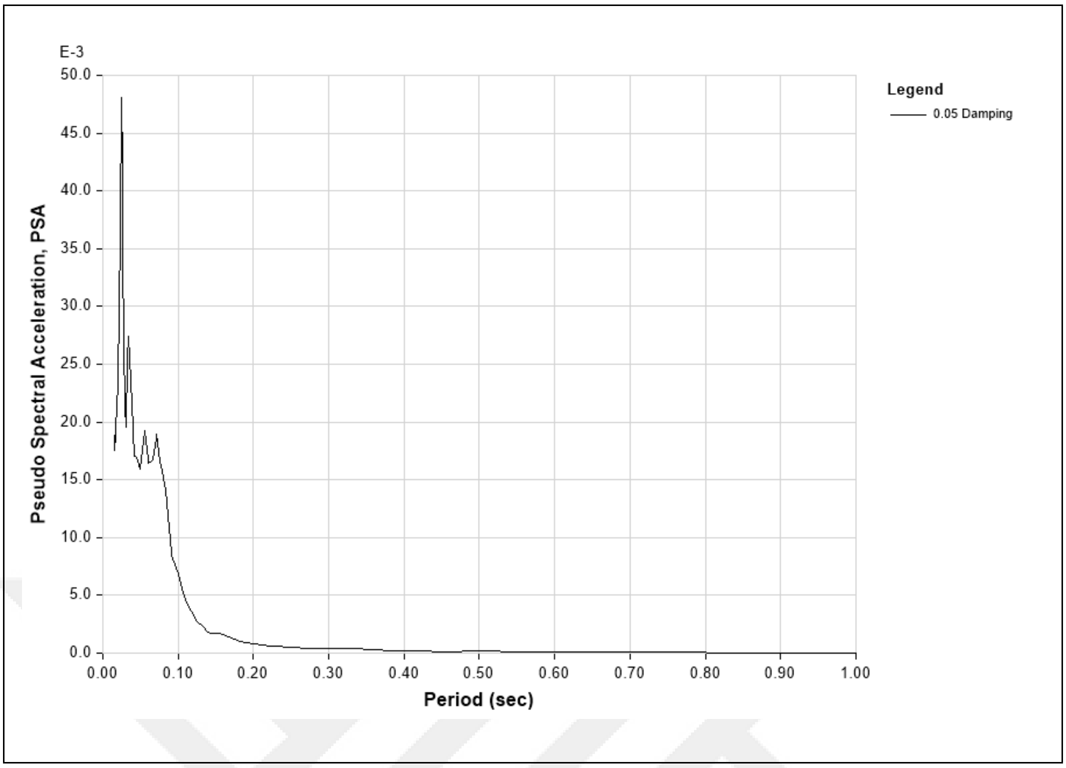

Figure 5.29: Vehicle 4B in X-Direction.

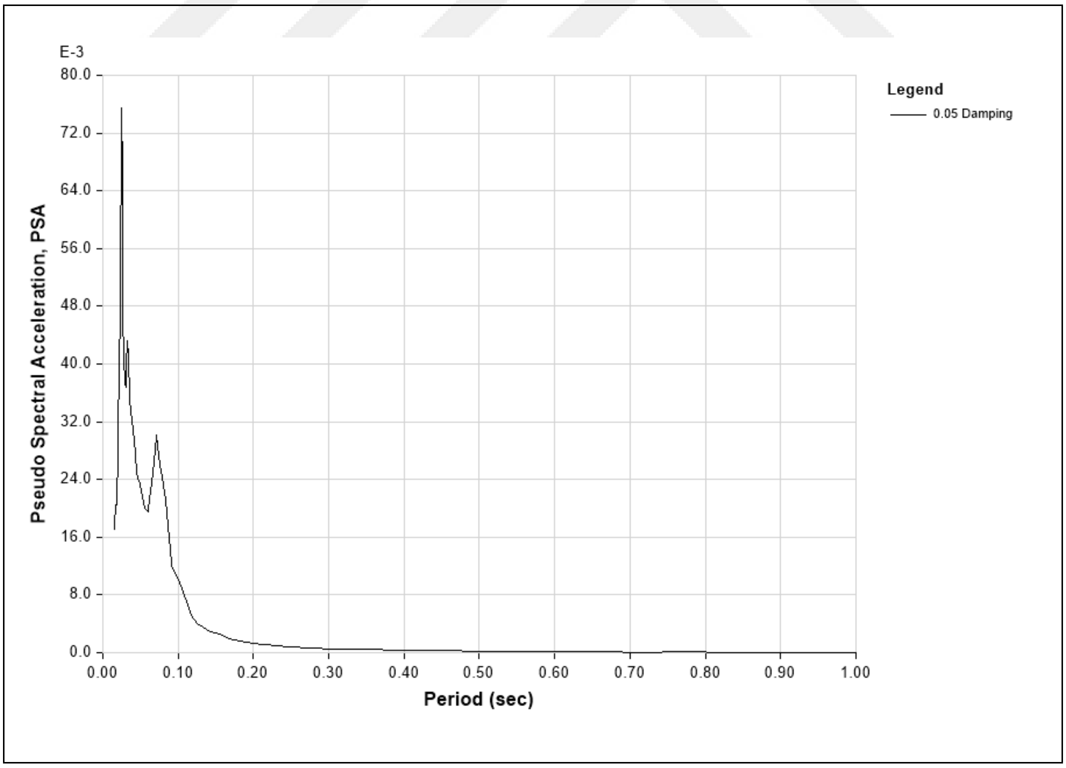

Figure 5.30: Vehicle 4B in Y-Direction.

The results of time history analysis on the seven minarets are shown in Table 5.6.

Table 5.6: Maximum Values of Time History Analyses Results.

Ground Motion	Minaret of	Mosque						
		Fatih	Yeni	Nusretiye	Yeni Valide	Little Hagia Sophia	Zeynep Sultan	Kepenekçi Sinan
Düzce Earthquake at Lamont 375	Top x-displacement (mm)	203.80	142.80	229.50	133.10	54.16	66.56	38.03
	Top y-displacement (mm)	193.40	141.10	229.50	177.50	70.31	78.04	82.64
	Top z-displacement (mm)	2.23	1.14	0.68	1.01	0.20	0.46	0.26
	Top x-velocity (mm/s)	2222.00	1720.00	2823.00	2539.00	757.30	790.00	573.60
	Top y-velocity (mm/s)	3273.00	3114.00	3426.00	4330.00	1171.00	1416.00	1261.00
	Top z-velocity (mm/s)	98.50	81.80	59.14	86.06	26.38	50.85	33.67
	Top x-acceleration (m/s^2)	63.40	56.17	130.50	101.20	24.56	30.62	18.40
	Top y-acceleration (m/s^2)	147.90	138.10	209.60	263.60	45.40	74.49	37.35
	Top z-acceleration (m/s^2)	8.82	7.99	7.01	10.72	3.56	4.95	5.02
	x stress (MPa)	7.48	6.03	9.17	2.70	1.43	1.51	1.72
	y stress (MPa)	9.50	5.39	9.10	3.34	1.31	1.53	1.88
	z stress (MPa)	18.44	20.06	25.44	8.24	3.88	6.23	4.09

Table 5.6: Maximum Values of Time History Analyses Results "Tables Continued".

Düzce Earthquake at Irigm 496	Top x-displacement (mm)	383.00	269.50	373.70	250.50	88.42	108.60	60.90
	Top y-displacement (mm)	168.50	217.60	315.50	212.70	84.89	141.00	71.34
	Top z-displacement (mm)	2.82	1.62	0.76	1.16	0.27	0.47	0.30
	Top x-velocity (mm/s)	3025.00	2302.00	4497.00	5030.00	1617.00	1495.00	1063.00
	Top y-velocity (mm/s)	3160.00	4329.00	5072.00	5316.00	1843.00	2304.00	1265.00
	Top z-velocity (mm/s)	158.30	64.73	34.87	75.06	26.09	27.27	23.17
	Top x-acceleration (m/s^2)	85.17	83.27	146.30	157.10	45.69	61.31	32.46
	Top y-acceleration (m/s^2)	96.33	127.40	162.50	163.50	52.35	106.20	31.32
	Top z-acceleration (m/s^2)	12.34	5.37	3.73	6.96	3.33	2.40	2.94
	x stress (MPa)	7.45	10.08	12.57	5.28	2.85	2.42	1.83
	y stress (MPa)	8.07	7.13	12.45	5.77	2.67	2.54	2.03
	z stress (MPa)	18.61	22.97	35.57	18.10	6.89	10.24	4.78
Düzce Earthquake at Bolu	Top x-displacement (mm)	483.00	506.10	480.70	823.30	314.50	585.20	210.40
	Top y-displacement (mm)	433.50	401.30	463.90	332.40	212.20	378.50	250.40
	Top z-displacement (mm)	2.22	1.14	0.62	2.50	0.31	0.47	0.35
	Top x-velocity (mm/s)	3832.00	3063.00	2944.00	7471.00	2771.00	4287.00	2193.00
	Top y-velocity (mm/s)	3256.00	2902.00	3520.00	4026.00	2603.00	2881.00	2634.00
	Top z-velocity (mm/s)	94.50	62.92	55.91	60.18	31.31	46.48	32.33
	Top x-acceleration (m/s^2)	59.83	45.80	75.55	91.04	38.20	38.74	27.14
	Top y-acceleration (m/s^2)	73.63	71.56	103.50	105.10	41.78	41.84	36.93
	Top z-acceleration (m/s^2)	7.85	5.60	6.63	7.08	4.56	5.10	4.41
	x stress (MPa)	8.81	10.36	6.84	6.57	5.10	4.37	5.84
	y stress (MPa)	9.53	9.69	6.83	6.66	5.33	6.27	6.01
	z stress (MPa)	20.16	25.88	19.41	22.11	17.22	25.78	13.96

Table 5.6: Maximum Values of Time History Analyses Results "Tables Continued".

Erzincan Earthquake at Erzincan	Top x-displacement (mm)	443.70	424.20	421.80	495.60	262.30	320.00	177.70
	Top y-displacement (mm)	808.20	748.30	884.00	421.10	187.80	431.90	127.00
	Top z-displacement (mm)	3.23	1.20	0.40	1.26	0.19	0.34	0.24
	Top x-velocity (mm/s)	2939.00	2378.00	2679.00	5062.00	2382.00	2528.00	1759.00
	Top y-velocity (mm/s)	3409.00	3475.00	4262.00	2764.00	1277.00	2586.00	899.70
	Top z-velocity (mm/s)	74.33	70.58	31.43	49.05	12.75	23.33	16.69
	Top x-acceleration (m/s^2)	45.70	45.96	54.40	86.78	34.35	24.60	29.75
	Top y-acceleration (m/s^2)	26.94	31.36	43.34	38.70	13.56	20.89	11.70
	Top z-acceleration (m/s^2)	6.31	6.00	3.13	4.85	1.68	2.34	2.12
	x stress (MPa)	14.07	17.10	11.07	4.33	3.76	5.36	4.55
	y stress (MPa)	16.67	11.83	11.30	4.36	4.21	4.02	4.76
	z stress (MPa)	33.05	39.07	32.31	14.30	14.02	18.34	12.89
Kocaeli Earthquake at Düzce	Top x-displacement (mm)	697.70	680.00	721.10	398.60	170.50	285.70	120.00
	Top y-displacement (mm)	337.40	228.40	304.10	245.90	139.80	220.90	135.50
	Top z-displacement (mm)	2.80	1.73	0.53	1.18	0.18	0.43	0.23
	Top x-velocity (mm/s)	2992.00	3396.00	3727.00	3588.00	1435.00	1971.00	1168.00
	Top y-velocity (mm/s)	2298.00	1921.00	2104.00	2416.00	1351.00	1514.00	1419.00
	Top z-velocity (mm/s)	114.20	85.07	43.65	62.75	15.69	36.22	17.53
	Top x-acceleration (m/s^2)	31.16	35.81	35.40	76.22	21.62	23.56	13.83
	Top y-acceleration (m/s^2)	29.29	24.29	38.16	35.91	19.72	20.93	17.84
	Top z-acceleration (m/s^2)	9.07	8.39	4.85	5.81	1.82	3.95	1.95
	x stress (MPa)	11.54	12.62	8.30	3.73	2.51	2.15	3.60
	y stress (MPa)	10.94	13.37	9.60	5.11	2.59	3.03	3.70
	z stress (MPa)	28.17	35.61	24.90	13.47	9.63	12.57	8.45

Table 5.6: Maximum Values of Time History Analyses Results "Tables Continued".

Kocaeli Earthquake at Yarimca	Top x-displacement (mm)	625.10	694.80	643.60	225.90	126.00	192.00	101.10
	Top y-displacement (mm)	297.00	363.80	328.90	282.20	179.90	172.50	128.30
	Top z-displacement (mm)	2.53	1.46	0.51	0.83	0.31	0.43	0.37
	Top x-velocity (mm/s)	3157.00	3021.00	3095.00	2155.00	1116.00	1101.00	962.40
	Top y-velocity (mm/s)	1357.00	2087.00	2075.00	2213.00	1696.00	1292.00	1232.00
	Top z-velocity (mm/s)	83.03	64.68	43.33	50.82	42.16	36.58	44.86
	Top x-acceleration (m/s^2)	28.47	28.90	29.05	41.72	10.74	17.46	10.91
	Top y-acceleration (m/s^2)	22.34	20.18	27.87	36.17	17.24	12.44	13.62
	Top z-acceleration (m/s^2)	8.12	6.30	4.74	5.55	5.83	3.87	6.17
	x stress (MPa)	10.65	15.93	7.25	2.20	2.89	2.05	3.14
	y stress (MPa)	10.16	13.84	8.34	3.00	2.81	2.20	3.22
	z stress (MPa)	26.40	36.51	22.13	7.02	9.12	9.20	6.87
Train 3A	Top x-displacement (mm)	0.14	0.12	0.17	0.24	0.05	0.19	0.05
	Top y-displacement (mm)	0.19	0.25	0.21	0.36	0.07	0.30	0.07
	Top z-displacement (mm)	0.03	0.03	0.03	0.04	0.02	0.02	0.03
	Top x-velocity (mm/s)	30.88	32.66	29.51	45.38	17.58	58.50	9.02
	Top y-velocity (mm/s)	36.58	53.25	53.43	61.00	21.53	97.08	12.05
	Top z-velocity (mm/s)	5.75	8.23	10.32	11.18	4.68	4.80	5.33
	Top x-acceleration (m/s^2)	7.94	10.35	9.37	13.17	7.69	20.36	3.63
	Top y-acceleration (m/s^2)	10.68	15.51	13.96	10.38	10.51	30.26	3.92
	Top z-acceleration (m/s^2)	1.36	2.32	3.20	2.90	1.53	1.88	1.66
	x stress (KPa)	33.13	28.26	109.10	32.10	17.85	18.96	38.32
	y stress (KPa)	35.58	46.94	161.34	45.01	21.15	53.56	74.00
	z stress (KPa)	54.25	86.90	129.95	74.11	48.00	74.49	74.90

Table 5.6: Maximum Values of Time History Analyses Results "Tables Continued".

Train 2C	Top x-displacement (mm)	0.11	0.08	0.13	0.19	0.09	0.26	0.03
	Top y-displacement (mm)	0.13	0.13	0.13	0.24	0.07	0.28	0.04
	Top z-displacement (mm)	0.03	0.03	0.02	0.03	0.03	0.02	0.02
	Top x-velocity (mm/s)	31.04	27.26	36.07	53.66	32.31	90.61	10.40
	Top y-velocity (mm/s)	31.38	41.29	39.07	47.92	24.29	79.51	11.90
	Top z-velocity (mm/s)	3.84	5.29	5.73	7.62	4.89	5.22	4.06
	Top x-acceleration (m/s^2)	10.82	9.80	12.77	17.16	14.43	31.39	6.27
	Top y-acceleration (m/s^2)	10.29	9.62	16.27	10.79	11.71	32.41	5.17
	Top z-acceleration (m/s^2)	1.34	1.67	2.30	2.24	1.51	2.21	1.32
	x stress (KPa)	21.14	21.61	141.74	16.13	17.86	19.74	43.69
	y stress (KPa)	32.62	47.27	178.00	29.73	29.15	48.40	58.86
	z stress (KPa)	45.26	53.45	143.50	46.47	48.92	67.88	101.93
Vehicle 4B	Top x-displacement (mm)	0.02	0.02	0.03	0.03	0.00	0.02	0.00
	Top y-displacement (mm)	0.02	0.03	0.04	0.05	0.01	0.02	0.01
	Top z-displacement (mm)	0.01	0.01	0.01	0.01	0.01	0.01	0.00
	Top x-velocity (mm/s)	3.25	2.14	3.84	4.30	0.81	2.90	0.52
	Top y-velocity (mm/s)	2.75	3.07	3.50	6.76	1.12	4.91	0.71
	Top z-velocity (mm/s)	0.93	0.86	0.92	1.01	0.83	0.64	0.74
	Top x-acceleration (m/s^2)	0.69	0.39	0.47	0.84	0.14	0.63	0.07
	Top y-acceleration (m/s^2)	0.55	0.69	0.54	1.15	0.23	1.08	0.16
	Top z-acceleration (m/s^2)	0.14	0.19	0.16	0.19	0.13	0.01	0.11
	x stress (KPa)	2.87	3.78	7.83	2.48	2.65	3.22	2.90
	y stress (KPa)	4.46	6.56	9.21	3.99	2.39	3.23	5.17
	z stress (KPa)	7.37	12.21	11.87	9.11	6.54	7.90	6.72

6. DISCUSSION AND CONCLUSION

6.1 EVALUATION OF THE FUNDAMENTAL PERIOD ESTIMATION EQUATIONS FOR MINARETS

As shown from (figure 5.1) to (figure 5.5) the correlation coefficients R in the regression analysis between the fundamental period and the material variables were few. The correlation coefficient R between the fundamental period and the material density approximately 0.6140, while the correlation coefficient R between the fundamental period and the modulus of elasticity is roughly equal to 0.6665, both are small percentages when we compared these results with the results of the correlation coefficients between the fundamental period and the geometric variables. According to the results, the correlation coefficient between the fundamental period and height is equal to 0.8848, the correlation coefficient between the fundamental period and cross section area is equal to 0.8388, and the correlation coefficient between the fundamental period and moment of inertia is equal to 0.8111. These correlation coefficients are higher percentages than the correlation coefficients with material variables.

To create an equation that contains the five variables, regression analysis was done between the fundamental period and the five variables (A, I, E, ρ, H). Another equation was developed by doing the regression analysis between the fundamental period and the two variables (H, I). The first equation includes both geometric and material characteristics which is given in Equation (5.1), whereas the second equation solely includes geometric variables as its given in Equation (5.2), therefore we have derived two equations to estimate the fundamental period.

T_2 represents the estimation of fundamental period produced by the two variables, whereas T_5 represents the fundamental period estimated by the five variables. E stands for the elastic modulus, ρ for material density, A for the cross section area at the bottom of the body, I for the moment of inertia at the bottom of the body and H represent the height, which is equal to the half-height of the boot section adding the height from the bottom of the transitional segment to the end of the spire section without adding the end ornament.

The Spire section is usually built either from stone or lead-coated wood. The Spire section has an important impact on the fundamental period because of its own weight, as it may reach almost 4000 kilograms. In addition to its height that can reach more than 11 meters, as it is in Fatih Mosque. The eliminating of the spire section could decrease the fundamental period approximately 15%. During the analysis the Spire section was taken into account and considered as a structural element in this study. The height of the Spire section was added to the total height of the minaret during the calculations. The reason for eliminating half the height of the boot section is that historically Ottoman minarets are usually constructed attached to some parts of the mosque, thus the stiffness of the minaret varies, so half the height of the boot will be more effective.

To evaluate the outcomes, it is necessary to fully understand the regression analysis outcomes. The correlation coefficient R represents how closely the independent variable is related to the dependent variable, while the determination coefficient R^2 shows how well the equation calculates the result of the dependent variable. The standard error is the arithmetic mean of the distances between the regression analysis points and the regression line.

The regression analysis was conducted in this study between the fundamental period and both the geometric properties variables and materials properties variables. The correlation coefficient R for the geometric properties was better than the correlation coefficients R for the material properties.

To examine the performance of the equations that were deduced during this study, the equations of this study and the equations of previous studies were applied to the seven minarets of this study and to 10 minarets of previous studies, the results are presented in Table 5.3. The results show that the fundamental period obtained from the equations in this study closely matches the reference period reported in previous studies. When comparing the results to the reference periods, the results of the two-variable equation (Equation 5.2) showed significantly better performance than the results of the five-variable equation determined in this study through regression analysis.

The 3-variable of Oliveira's equation gave results that can be comparable with the reference period, on the other hand the equations of Serhatoğlu and Livaoğlu with 3-variable and 5-variable decreased the value of the reference period. The equations with one variable had similar results, which might be explained by the fact that the variable in all equations is the same, which is height. The best equation with one variable was the Shakya equation.

In this study, multiple equations were applied to estimate the fundamental period for minarets. The two equations derived from this study, the Oliveira's equation, the two equations proposed by Serhatoğlu and Livaoğlu, as well as four equations with a single variable (Faccio et al, Rainieri and Fabbrocino, Ministerio de Fomento, and Shakya). These equations were applied to both the seven minarets from this study and to the ten minarets from previous studies. The equation that includes two variables Equation (5.2), namely height and moment of inertia produced the best results.

6.2 DYNAMIC BEHAVIOR AND MPMR OF MINARETS

Modal analysis is a technique for studying the dynamic behavior of structures. It also aids in understanding how the structure will vibrate and respond. The results of modal analysis for many mosque minarets provide insight into their dynamic behavior. Starting with the seven minarets' mode shapes, the first and second modes have sway shapes, which indicates lateral movement. The third and fourth modes have lateral bending shapes, indicating bending deformation. The fifth mode of Fatih Mosque, Yeni Mosque, Nusretiye Mosque, and Yeni Valide Mosque have a series bend shape, which indicates more complex bending patterns, however torsional motion is represented in the fifth mode in Little Hagia Sophia Mosque, Zeynep Sultan Mosque, and Kepenekçi Sinan Mosque. The sixth mode of the Fatih Mosque and Yeni Valide Mosque have torsional motion, indicating structure twisting, while the Yeni Mosque, Nusretiye Mosque, Little Hagia Sophia Mosque, Zeynep Sultan Mosque, and Kepenekçi Sinan Mosque show a series bend shape. Fatih Mosque, Yeni Mosque, Nusretiye Mosque, Yeni Valide Mosque, Little Hagia Sophia Mosque, Zeynep Sultan Mosque, and Kepenekçi Sinan Mosque exceed the 90% Modal Participating Mass Ratio in both the sum of UX and the sum of UY directions at 33rd, 35th, 53rd, 37th, 21st, 144th, and 97th modes, respectively.

6.3 VERTICAL STRESS DISTRIBUTION OF VARIOUS MOSQUE MINARETS

a. Minaret of Fatih Mosque

The minaret of Fatih Mosque was analyzed under the effect of self-weight load, and the total self-weight was estimated as 19928 kN based on the materials shown in Table 4.2. The vertical stresses in the minaret's Spire section are very low, with the highest value measured at the base of the spire being approximately 0.07 MPa. The vertical stresses along the height of the polygonal body steadily rise from top to bottom, with values ranging from 0.07 MPa to 1.00 MPa. The vertical stresses at the transition segment steadily drop from 1.00 MPa at the top of the segment to 0.63 MPa at the bottom of the segment as the cross-section area of the transition segment increases at the bottom. Vertical stresses increase from 0.63 MPa at the top of the boot section to 1.46 MPa at the base of the minaret. (Figure 5.6) shows the vertical stresses and deformed shape of Fatih Mosque's minaret.

b. Minaret of Yeni Mosque

Based on the materials in Table 4.2, the weight of the Yeni Mosque's minaret was determined to be 11160 kN. The vertical stresses in the minaret's Spire section are extremely low, with the highest value observed at around 0.06 MPa at the base of the spire section. Along the height of the polygonal body, vertical stresses vary from 0.06 MPa at the top of the polygonal body to 1.00 MPa at the bottom of the polygonal body. The vertical stresses at the transition segment steadily drop from 1.00 MPa at the top of the segment to 0.30 MPa at the bottom of the segment, due to the increasing of the cross-section area at the bottom of the transition segment. Vertical stresses rise from 0.30 MPa to 1.45 MPa in the boot section. (Figure 5.7) presents the vertical stresses and deformed shape of Yeni Mosque's minaret.

c. Minaret of Nusretiye Mosque

The overall weight of the minaret of Nusretiye Mosque is calculated to be 5768 kN according to the materials in Table 4.2. The vertical stresses in the Spire section of the minaret are significantly low, with the greatest value measured at roughly 0.08 MPa at the bottom of the spire section. Vertical stresses along the polygonal body range from 0.08 MPa to 0.90 MPa. The transitional segment of the minaret is pear-shaped, and the vertical stresses have not changed because the upper and lower diameters are the same. In the boot section, vertical stresses rise from 0.90 MPa to 1.84 MPa. (Figure 5.8) presents the vertical stresses and deformed shape of Nusretiye Mosque's minaret.

d. Minaret of Yeni Valide Mosque

The minaret of the Yeni Valide Mosque was tested under the effect of self-weight load, and the total self-weight was measured as 3725 kN. The vertical stresses in the minaret's Spire section are quite low, with the highest value found at around 0.07 MPa at the base of the spire section. The vertical stresses in the polygonal body rise consistently from top to bottom, with values ranging from 0.07 MPa to 0.5 MPa. The vertical stresses at the transition segment drop steadily from 0.5 MPa at the top to 0.25 MPa at the bottom as the cross-section area of the transition segment increases at the bottom. Vertical stresses increase from 0.25 MPa at the top of the boot section to 0.75 MPa at the bottom of the minaret. (Figure 5.9) shows the vertical stresses and deformed shape of Yeni Valide Mosque's minaret.

e. Minaret of Little Hagia Sophia Mosque

Under the effect of self-weight load, the Minaret of Little Hagia Sophia was analyzed by using the materials in Table 4.2. The total self-weight was determined as 1870 kN. The vertical stresses in the Spire section of the minaret are relatively low, with the greatest value observed at roughly 0.04 MPa. The vertical stresses in the polygonal body gradually increase from the top to the bottom, with values ranging from 0.2 MPa to 0.45 MPa. As the cross-section area of the transition segment rises at the bottom, the vertical stresses at the transition segment decrease continuously from 0.45 MPa to 0.2 MPa. Vertical stresses increase from 0.2 MPa at the boot section's top to 1.14 MPa at the minaret's base. (Figure 5.10) describe the vertical stresses and deformed shape of Little Hagia Sophia Mosque's minaret.

f. Minaret of Zeynep Sultan Mosque

The minaret of the Zeynep Sultan Mosque was examined under self-weight load, and its overall self-weight was estimated to be 1700 kN. The vertical stresses in the Spire section of the minaret are extremely small, having the greatest value measured at roughly 0.04 MPa at the bottom of the spire section. The vertical stresses in the polygonal body rise from top to bottom, with values varying from 0.04 MPa to 0.42 MPa. As the transition segment's cross-section area increases, the vertical stresses at the transition segment decrease continuously from 0.42 MPa to 0.07 MPa. Vertical stresses vary from 0.07 MPa at the top of the boot sections to 1.61 MPa at the bottom of the minarets. (Figure 5.11) describe the vertical stresses and deformed shape of Zeynep Sultan Mosque's minaret.

g. Minaret of Kepenekçi Sinan Mosque

The minaret of Kepenekçi Sinan Mosque was studied under the effect of self-weight load, and its total self-weight was found to be 1146 kN. The vertical stresses in the minaret's Spire section are quite small, with the highest value found at roughly 0.02 MPa at the bottom of the spire section. The vertical stresses in the polygonal body are continually increasing from top to bottom, with values that range from 0.02 MPa to 0.26 MPa. The vertical stresses at the transition segment fall gradually from 0.26 MPa to 0.07 MPa as the cross-section area of the transition segment increases. Vertical stresses rise from 0.07 MPa at the top of the boot section to 1.22 MPa at the base of the minaret. (Figure 5.12) describes the vertical stresses and deformed shape of Kepenekçi Sinan Mosque's minaret.

Finally, the self-weight analysis of numerous mosque minarets has been conducted, and the stress values under self-weight load has been analyzed and listed in Table 5.5. Typically, the spire sections of the minarets exhibit minimal vertical stresses, while gradual increases are observed along the height of the polygonal bodies. The vertical stress values in the transition segments vary due to differences in cross-sectional areas. The boot sections have the highest vertical stresses, reaching their peak values at the bases of the minarets. This understanding assists in the design and evaluation of these structures.

6.4 EVALUATION THE SEISMIC RESPONSE OF MINARETS UNDER DIFFERENT GROUND MOTIONS

When examining the impact of earthquakes on the minaret of Fatih Mosque, specifically the Düzce Earthquake at Irigm 496 and the Kocaeli Earthquake at Yarimca, it was observed that the maximum stress values recorded were 18.61 MPa and 26.40 MPa, respectively. The disparity in stress levels between these two earthquakes can be attributed to the Kocaeli Earthquake at Yarimca having nearly twice the spectral acceleration compared to the Düzce Earthquake at Irigm 496 in the first mode, in the east-west (X) direction, with a mass participation ratio of 11.88%. Similarly, when analyzing the minaret of Yeni Mosque under the influence of the Düzce Earthquake at Bolu and the Erzincan Earthquake at Erzincan, the highest stress values recorded were 25.88 MPa and 39.07 MPa, respectively. The variation in stress levels between these two earthquakes can be attributed to the Erzincan Earthquake having nearly twice the spectral acceleration of the Bolu Earthquake in the first mode, specifically in the north-south (Y) direction, with a mass participation ratio of 13.38%. Furthermore, when investigating the minaret of Zeynep Sultan Mosque and its response to the Train 2C and Train 3A ground motion, the highest stress values recorded were 67.88 KPa and 74.49 KPa, respectively. The difference in stress levels between these two train vibrations can be attributed to Train 3A having a spectral acceleration that was 50 percent greater than Train 2C in the first mode, specifically in the north-south (Y) direction. The mass participation ratio was found to be 15.22%. Lastly, the analysis of the minaret of Kepenekçi Sinan Mosque under the influence of Train 2C and Vehicle 4B revealed maximum stress values of 101.93 KPa and 6.72 KPa, respectively. The discrepancy in stress levels between these two ground motions can be attributed to Train 2C having approximately five times the spectral acceleration compared to Vehicle 4B. This variation was specifically observed in the first mode, in the east-west (X) direction, with a mass participation ratio of 13.71%.

Overall, the examination of these minarets under different seismic events and ground motion recordings highlights the varying stress levels, primarily influenced by the spectral acceleration and direction of the first mode, along with the corresponding mass participation ratio.

REFERENCES

[1] İrfan Üstündağ, Hakkı Alçep, Erdal Karaman, 2017, Fatih Camileri ve Mescidleri (Mosques and Masjids in Fatih), Publication of Fatih Müftülüğü, Türkiye Diyanet Vakfı (Türkiye Religious Foundation).

[2] Dursun ARSLAN, (2018), Tarihsel Konumu ve mimarisiyle Nusretiye Camii, Issue 13, 2018, pp.53 - 85, https://doi.org/10.34242/akmbaris.2019.79

[3] Ahmet Ersen, Technical Report, the type and conditions of natural stones used in the construction of the minarets of Yeni Mosque, Project No:03.10.089, Date: 12.11.2003, İstanbul Technical University, Faculty of Architecture.

[4] Erkal A., 2022, Response of Little Hagia Sophia (Church of SS Sergius and Bacchus) to adjacent Train-induced Vibrations, ACM Journal on Computing and Cultural Heritage, Vol. 15, No. 3, Article 54.

[5] Eser Çaktı, Carlos S. Oliveira, Jose V. Lemos, Özden Saygılı, Serkan Görk and Esra Zengin EARTHQUAKE BEHAVIOR OF HISTORICAL MINARETS IN ISTANBUL COMPDYN 2013 4th ECCOMAS Thematic Conference on Computational Methods in Structural Dynamics and Earthquake Engineering M. Papadrakakis, V. Papadopoulos, V. Plevris (eds.) Kos Island, Greece, 12–14 June 2013.

[6] Cavit Serhatoğlu, Ramazan Livaoğlu, 2019, A fast and practical approximations for fundamental period of historical Ottoman minarets, Soil Dynamics and Earthquake Engineering, pp.320-331.

[7] P. Faccio, S. Podest`a, A. Saetta, A. Venezia, 2009, Campanile della Chiesa di Sant'Antonio, Esempio 5., Linee guida per la valutazione e riduzione del Rischio Sismico del Patrimonio Culturale Allineate alle Nuove Norme Tecniche per le Costruzioni (DM 14/01/2008), Roma (in Italian).

[8] Rainieri, C., and G. Fabbrocino. 2011. Predictive correlations for the estimation of the elastic period of masonry towers. In Proceedings of Experimental Vibration Analysis for Civil Engineering Structures (EVACES 2011) (October 3–5, 2011, Varenna, Italy), 513–520.

[9] Ministero delle Infrastrutture e dei Trasporti, Nuove Norme Tecniche per le Costruzioni, NTC 2008, D.M. del Ministero delle Infrastrutture e dei Trasporti del 14/01/2008. G.U. n. 29 del 04.02.2008, S.O. n. 30, Roma (in Italian), 2008.

[10] M. Shakya, H. Varum, R. Vicente, and A. Costa, 2016, Empirical Formulation for Estimating the Fundamental Frequency of Slender Masonry Structures, International Journal of Architectural Heritage, Vol 10, No 1, pp.55–66.

[11] Fanmeng Kong, Yiguo Xue, Daohong Qiu, Huimin Gong, Zexu Ning, 2021, Effect of grain size or anisotropy on the correlation between uniaxial compressive strength and Schmidt hammer test for building stones, Construction and Building Materials, Vol.299, pp.1-12.

[12] Katz, O., Z. Reches, and J. Roegiers. 2000. Evaluation of mechanical rock properties using a Schmidt Hammer. International Journal of Rock Mechanics and Mining Sciences 37 (2000):723–728.

[N] Ahmet Ersen, Technical Report, the type and conditions of natural stones used in the construction of the minarets of Yeni Mosque, Project No:03.10.089, Date: 12.11.2003, İstanbul Technical University, Faculty of Architecture.

[13] Smith, M. R., ed. 1999. Stone: Building stone, rock fill and armourstone in construction. Geological Society, 16. London, UK: Engineering Geology Special Publications.

[14] R. C. de Vekey. 1990. Maintenance of brick and stone masonry structures, A. M. Sowden (Ed.) Chapman and Hall, London, 1990, 25–31.

[15] BSI (British Standards Institution) (2005). “Code of practice for the use of masonry — Part 2: Structural use of reinforced and prestressed masonry.” *BS 5628-2:2005*, London, UK.

[16] A. Bayraktar, A. C. Altunisik, B. Sevim, and T. Turker, 2011, Seismic Response of a Historical Masonry Minaret using a Finite Element Model Updated with Operational Modal Testing, Journal of Vibration and Control, Vol 17, No 1, pp.129–149.

[17] F. Tresnjo, M. Humo, F. Casarin, and N. Ademovic, 2023, Experimental Investigations and Seismic Assessment of a Historical Stone Minaret in Mostar, *Buildings,* Vol 13, No 2, p536. 34p.

[18] Y. S. Erdogan, T. Kocatürk, and C. Demir, 2019, Investigation of the Seismic Behavior of a Historical Masonry Minaret Considering the Interaction with Surrounding Structures, Journal of Earthquake Engineering, Vol 23, No 1, pp.112–140.

[19] A. Dogangun, R. Acar, H. Sezen, and R. Livaoglu, 2008, Investigation of dynamic response of masonry minaret structures, Bulletin of Earthquake Engineering, Vol 6, No 6, pp.505–517.

[20] A. Bayraktar, and E. Hokelekli, 2020, Influences of earthquake input models on nonlinear seismic performances of minaret-foundation-soil interaction systems, Soil Dynamics and Earthquake Engineering, Vol 139, pp.1–21.

[21] M. Yurdakul, F. Yılmaz, M. Artar, O. Can, E. Oner, and A. T. Daloglu, 2021, Investigation of time-history response of a historical masonry minaret under seismic loads, Structures, Vol 30, pp.265–276.

[22] K. Hacıefendioglu, G. Demir, and E. Alpaslan, 2016, Determination of Modal Parameters of Historical Masonry Minarets by using Operational Modal Analysis, Conference Proceeding of the World Congress on Civil, Structural, and Environmental Engineering (CSEE'16) Prague, Czech Republic, March 30 – 31, 2016 Paper No. ICSENM 104.

[23] E. Isık, F. Avcil, E. Harirchian, E. Arkan, H. Bilgin, and H. B. Ozmen, 2022, Architectural Characteristics and Seismic Vulnerability Assessment of a Historical Masonry Minaret under Different Seismic Risks and Probabilities of Exceedance, Buildings, Vol 12, No 8, pp.1–32.

[24] R. Livaoglu, M. H. Basturk, A. Dogangun, and C. Serhatoglu, 2016, Effect of Geometric Properties on Dynamic Behavior of Historic Masonry Minaret, KSCE Journal of Civil Engineering, Vol 20, No 6, pp.2392–2402.